A Gravity Investigation of the Tobacco Root Batholith Southwest Montana

Stephen Charles Tatum
Western Michigan University

A GRAVITY INVESTIGATION OF THE TOBACCO ROOT BATHOLITH SOUTHWEST MONTANA

Stephen Charles Tatum, M.S.

Western Michigan University, 2015

The objective of this research was to delineate and profile the Late Cretaceous Tobacco Root batholith in southwestern Montana through the application of the gravitational method. This survey was accomplished by obtaining 232 gravity measurements in four profiles across the batholith. After correcting for known variations in the gravity field, a Bouguer anomaly map of the batholith and surrounding host rocks was created. Four residual gravity profiles and map, created by subtracting the regional gravity from the Bouguer anomaly, reveal a maximum negative gravity anomaly in the center portion of the batholith which is parallel to the trend of the batholith. The batholith consists of granitic rocks that have measured densities that are 0.20 g/cm^3 smaller than the Precambrian (Archean) metamorphic rocks into which they are intruded. This density contrast produced negative gravity anomalies up to -46.7 mGal. Modeling of the profiles using measured densities indicates that the batholith extends to its greatest depth (20 km) in the subsurface. Another gravity low on the northwest, near the Jefferson River, suggests a subsurface extension of the batholith in that direction. The modeled profiles also suggest a decrease in depth and lateral extent from the center portion of the batholith to the southeast. The narrow subsurface shape on the northwest, parallel to the principal faults, the rapid thickening toward the central region, and the abrupt termination on the southeast are compatible with magma movement from the northwest.

A GRAVITY INVESTIGATION OF THE TOBACCO ROOT BATHOLITH SOUTHWEST MONTANA

by

Stephen Charles Tatum

A thesis submitted to the Graduate College
in partial fulfillment of the requirements
for the degree of Master of Science
Geosciences
Western Michigan University

May 2015

Thesis Committee:

Christopher Schmidt, Ph.D., Chair
William Sauck, Ph.D.
Ronald Chase, Ph.D.

ACKNOWLEDGMENTS

I would like to extend sincere thanks to a number of people that contributed to this project and to the ones that conveyed moral attributes in the completion of my Masters thesis project. First and foremost I would like to thank Dr. Christopher Schmidt for coming to me with the proposal to extend in his research in the Tobacco Root Batholith and for his leadership and expertise, both in the field and in the lab. He conveyed certain qualities and methods towards this project that made it fun, exciting, interesting and he inflicted a drive in me that helped keep my focus on the completion of this project. I couldn't have done it without you, buddy. I would like to thank Dr. William Sauck for his knowledge, expertise and time during the completion of this research. He exerted special attributes in the reduction of my data, software usage and in equipment operations. I would like to thank Dr. Ronald Chase for his expertise in petrology, which aided in the identification of different lithologies. I would like to thank Theodore Bornhorst from Michigan Technological University for his work on density determination by Pycnometer for the lithology samples acquired in the field. I would like to thank Montana Bureau of Mines and Geology for providing me with the maps I needed in order to complete this project. I would like to thank Travis Hayden for his time and expertise in the operations of field equipment used during this project. I would like to thank Mohammad El-Sayed Ahmed for his contributions during post processing, particularly with terrain corrections and other software attributes. I would like to thank Gene Schmidt for his assistance field data collection. I would, again, like to thank Dr. Christopher Schmidt for his hospitality

while in Montana collecting field data. And lastly, but certainly not least, I would like to thank my friends and family for all their patience and support during the completion of this project. Thank you all.

Stephen Charles Tatum

TABLE OF CONTENTS

Table of Contents—continued

Table of Contents—continued

LIST OF TABLES

LIST OF FIGURES

List of Figures—continued

CHAPTER I

INTRODUCTION

Purpose and Methodology

The Boulder and the Tobacco Root batholith are the most eastern group of a wide belt of batholiths that are thought to be associated with the Mesozoic subduction of the oceanic (Farallon) plate beneath the continental North American plate (Schmidt et al. 1990). The Boulder batholith was emplaced into Middle Proterozoic (Belt Supergroup) rocks of the Helena structural salient of the Cordilleran thrust belt (Figure 1) as thrust faulting was taking place. The Tobacco Root batholith is the largest satellite pluton of the Boulder batholith but was emplaced entirely within the Archean metamorphic basement rocks of the Rocky Mountain foreland during oblique left-lateral movement on a set of northwest trending faults. Schmidt et al. (1990) suggested that intrusion was aided by the creation of one or more pull-apart zones between the basement faults.

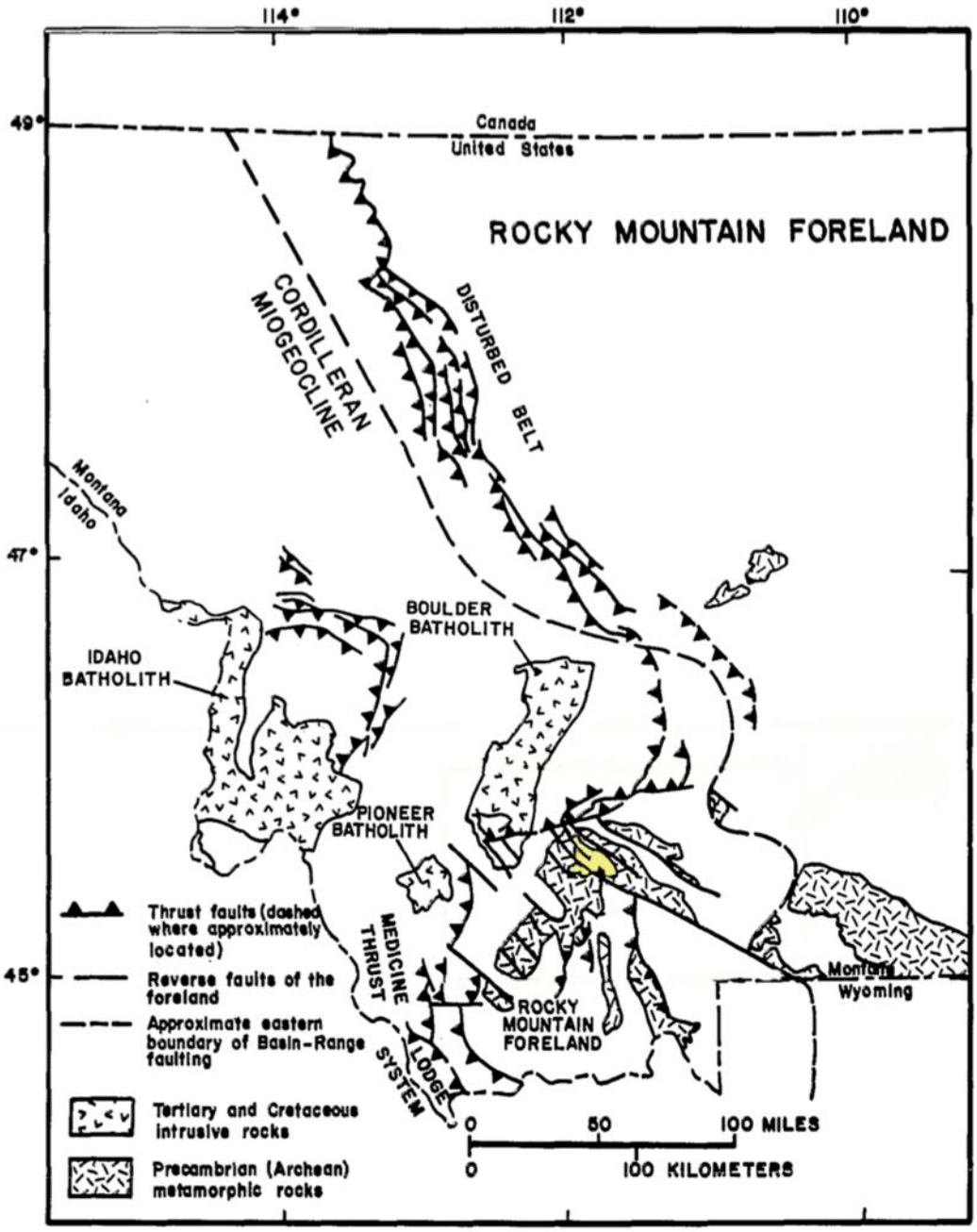

Figure 1: Schematic map of southwestern Montana depicting various fault trends and the Idaho, Boulder and Pioneer batholiths. The Tobacco Root batholith is highlighted in yellow surrounded by Precambrian (Archean) metamorphic rocks (Modified from Schmidt and Hendrix, 1981).

The primary objective of this study is to determine the subsurface shape of the Tobacco Root batholith using gravity data. This may permit a better understanding of the mode of emplacement of the batholith. The surface geometry and the lithologies of the batholith are well known from geologic maps (Smith, 1977 and Vitaliano et al. (2004), but the subsurface geometry is not well known or understood. The subsurface geometry from gravity may help determine the extent to which faults have controlled the intrusion of the batholith.

The way in which batholiths are emplaced into the crust is one of the most enduring problems in geology. Batholiths are typically found at or near converging plate margins and vary greatly in size and shape depending largely on depth, surrounding geology, physical properties of the subsurface, and mode of emplacement. Ever since Pitcher's (1978) work on the Peruvian batholith, it has been recognized that batholiths at converging margins are emplaced into zones of extension. How zones of extension are created is now thought to be related to rollback of a subducting plate. What makes the Boulder batholith and Tobacco Root batholith different is that emplacement was into areas of crustal shortening. The most recent model proposed for the mechanism of emplacement of the Tobacco Root batholith suggests the northwest trending faults that cut through the batholith and the Archean metamorphic host rocks played an active role by providing one or more extensional pull-apart zones for the progressive emplacement of felsic magma. In order to test this or any hypotheses of emplacement, the subsurface geometry of the batholith and faults should be known within reasonable limits.

The Tobacco Root batholith and Boulder batholith show evidence of being intruded into a region of coeval thrusting. The Tobacco Root batholith, for example, shows evidence of emplacement while the northwest trending faults that transect the

batholith were actually moving (Schmidt et al. 1990). Guineberteau et al. (1987) and Hutton (1988) proposed a mechanism in which space is made in the process of compression by wrench fault movement similar to the way pull-apart basins are produced. From this, Schmidt et al (1990) hypothesized that a similar pull-apart mechanism may be applied to the emplacement of the Tobacco Root batholith. This hypothesis remains to be tested. Knowledge of the subsurface geometry and delineation of the batholith is a critical test in the interpretation of mode of emplacement.

In order to make a gravity interpretation of the subsurface of the Tobacco Root batholith, a number of gravity stations must be established along transects perpendicular to the strike of the batholith with readings taken outside the contact of the batholith and extending into the batholith at appropriate intervals. A number of factors need to be considered when collecting gravity data. When collecting gravity data, position (especially latitude) needs to be known. This will be discussed in more detail in Chapter III, (Data Collection and Reduction). Corrections need to be made for: instrument drift, local topography (terrain), and elevation.

Previous Work

Burfeind (1967) performed a gravity investigation of the Tobacco Root Mountains, Jefferson Basin, Boulder batholith, and adjacent areas of southwestern Montana. Burfeind interpreted the Tobacco Root batholith as an asymmetric tabular body whose northeastern contacts dip steeply to the southwest, and whose northwest and southeast contacts dip towards each other at low angles before dipping steeply northwest (Burfeind 1967). Burfeind's work shows a relationship between the Boulder batholith and the Tobacco Root batholith. He interpreted the Boulder

batholith to have a flat or concave upward floor and a depth of 8 to 10 km from the surface on a basis of 0.18 g/cm^3 density contrast. A reasonable gravity model (Figure 2) with a density contrast of 0.10 g/cm^3 suggests a thicker batholith and places the base of the batholith at a depth of 17 km (Schmidt et al. 1990). Smith's (1977) work described the Tobacco Root batholith with emphasis on petrographic characterization and geographic delineation of each rock type. The batholith is composed of granitic rocks and is evaluated quantitatively in the variations of different rock types within the batholith. Vitaliano et al. (2004) compiled a map of the Archean metamorphic rocks and Cretaceous batholith rocks as well as other igneous rocks of Proterozoic and late Mesozoic age in the Tobacco Root Mountains.

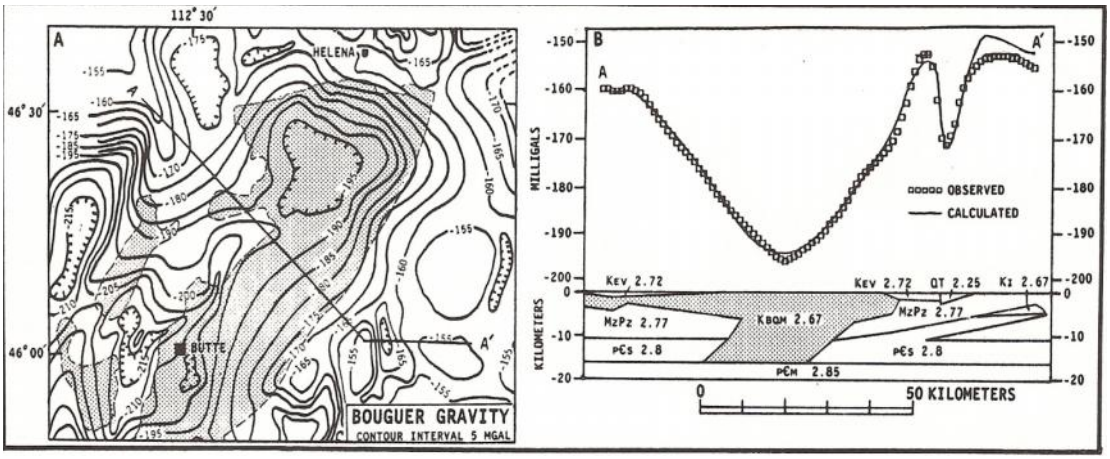

Figure 2: A) Burfeind (1967) Bouguer anomaly map and a B) gravity profile (Schmidt et al. 1999) over the central portion of the Boulder batholith with a depth of 8 to 10 km from the surface on a basis of 0.18 g/cm3 density contrast, and a flat and concave upward floor.

Area of Study

The Tobacco Root batholith lies in the Tobacco Root Mountains in southwest

Montana. The survey area was conducted in Madison County including the 7.5' topographic map series of; Manhead Mountain, Pony, Harrison, Noble Peak, Potosi Peak, Maltbys Mound, Noris, Copper Mountain, Ramshorn Mountain, Leonard Creek and Ennis Lake (Figure 3). The geographical area covered by this survey lies between latitudes 45° and 46° and longitudes 111° and 112°. The total area of the survey and the batholith is approximately 310 km^2 and extends beyond the contacts of the batholith in the northeast and southwest direction by about 1km to 2km. A total of four SW-NE trending transects were surveyed perpendicular to the NW-elongate trend of the batholith and one transect in a NW direction along "strike" perpendicular to the four SW-NE -trending transects (Figure 3).

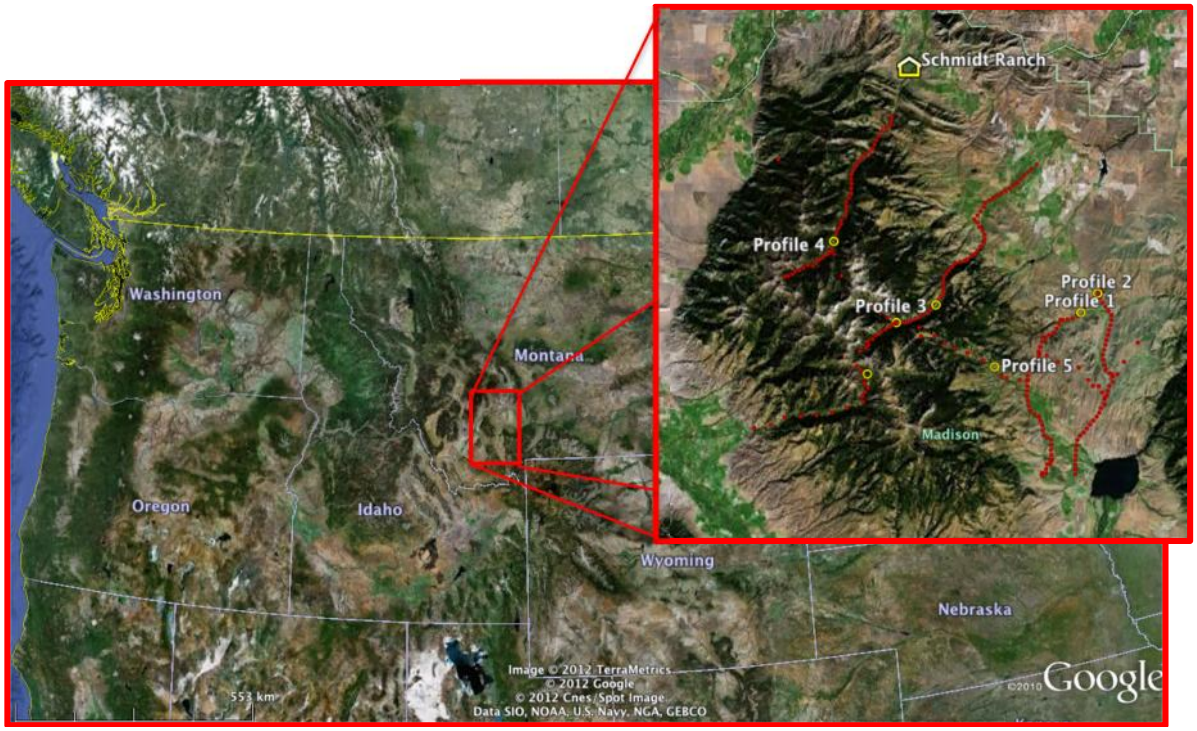

Figure 3: Survey area of the Tobacco Root Mountains over the Tobacco Root Batholith. The dotted red lines indicate each gravity station with yellow circles as base stations for each individual transect.

CHAPTER II

GEOLOGY OF THE TOBACCO ROOT MOUNTAINS

Introduction

The gravity survey conducted for this project covers most of the northern half of the Tobacco Root Mountains and extends beyond the mountain range to the east. The batholith is located in the central portion of the Tobacco Root Mountains and has a northwest-southeast trend (Figure 4). The northwest portion of the batholith (Hollow Top Mountain) has the highest elevation in the range (10,604 feet). One of the major structural features is a northwest- trending fault set that consists of four major faults (Schmidt and Garihan, 1986): The Carmichael/Pony fault, Mammoth fault, Hollow Top fault, and Bismark/North Meadow Creek fault (Figure 4). These northwest trending faults all dip steeply northeast and have had at least three distinct periods of movement: 1) Middle to Late Proterozoic normal faulting (Schmidt and Garihan, 1986); 2) Laramide (Late Cretaceous to Paleocene) left-reverse oblique slip producing west-east shortening; and 3) Neogene right-hand normal slip during east-west Basin-Range extension (Schmidt and Garihan, 1986). The Late Cretaceous movement is thought to have controlled the emplacement of the Tobacco Root batholith into the Archean basement rocks (Schmidt et al 1990).

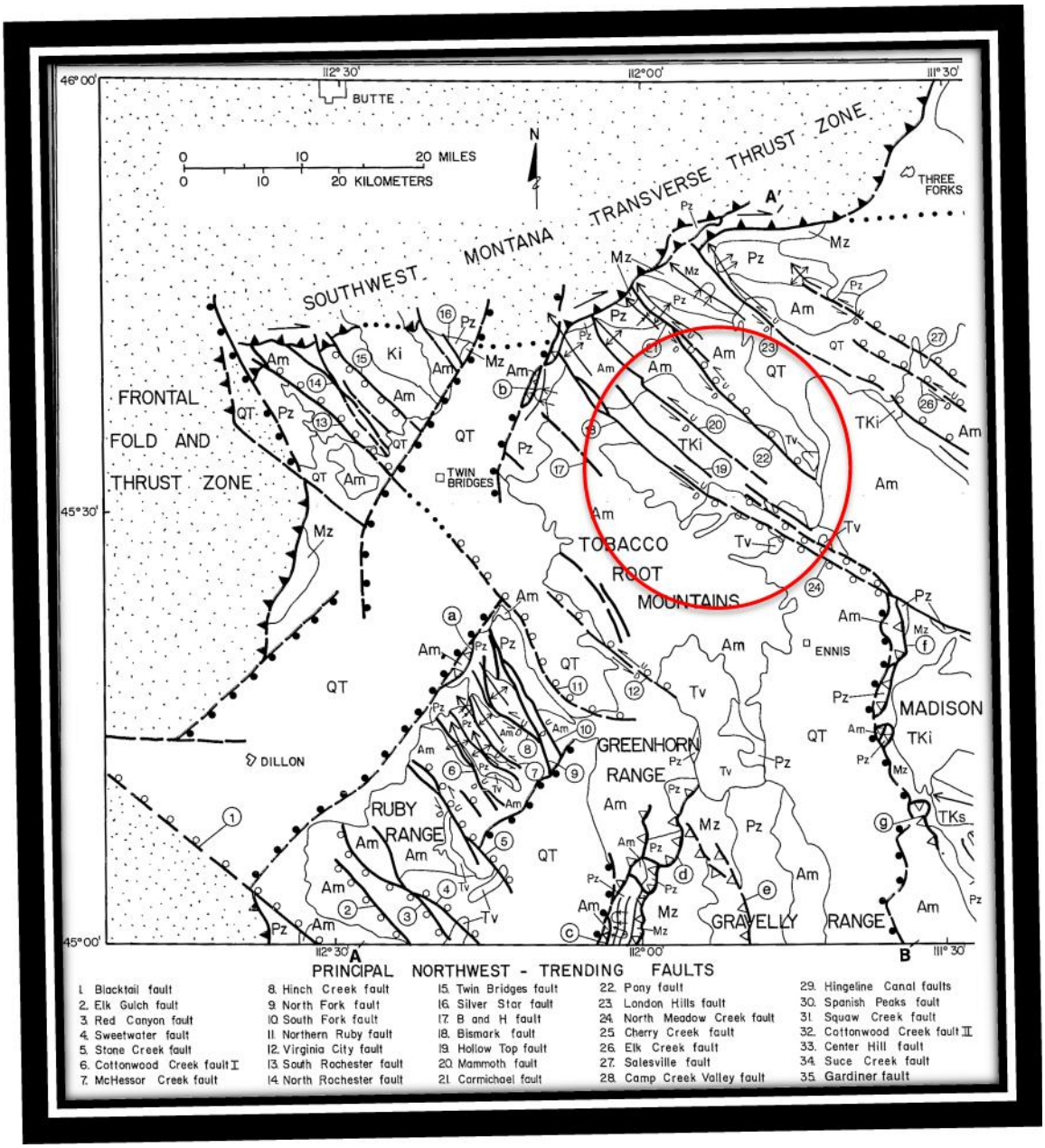

Figure 4: Tectonic map of the foreland depicting the northwest trending faults that cut through the Tobacco Root Batholith (outlined in red). (Schmidt and Garihan, 1986)

Tectonic History and Fault Movement

Proterozoic

The Mammoth and Bismark faults show evidence of Precambrian movement, first proposed by Reid (1957) and later confirmed by maps produced by Vitaliano et al, 1979; and Schmidt and Garihan, 1986. The map (Figure 5) produced by Schmidt and Garihan (1986) shows the Mammoth fault having right-lateral separation of a marble unit in Archean rocks by nearly 3.5 km but left-lateral separation of the Cambrian-Archean boundary by approximately 200 meters (Schmidt and Garihan, 1986). Separation of Archean units is also evident along the Bismark fault. The separations of the Archean metamorphic rock units differ a great deal from separations of Paleozoic sedimentary rocks, indicating that initial movements took place in (post Archean) Precambrian time (Schmidt and Garihan, 1983).

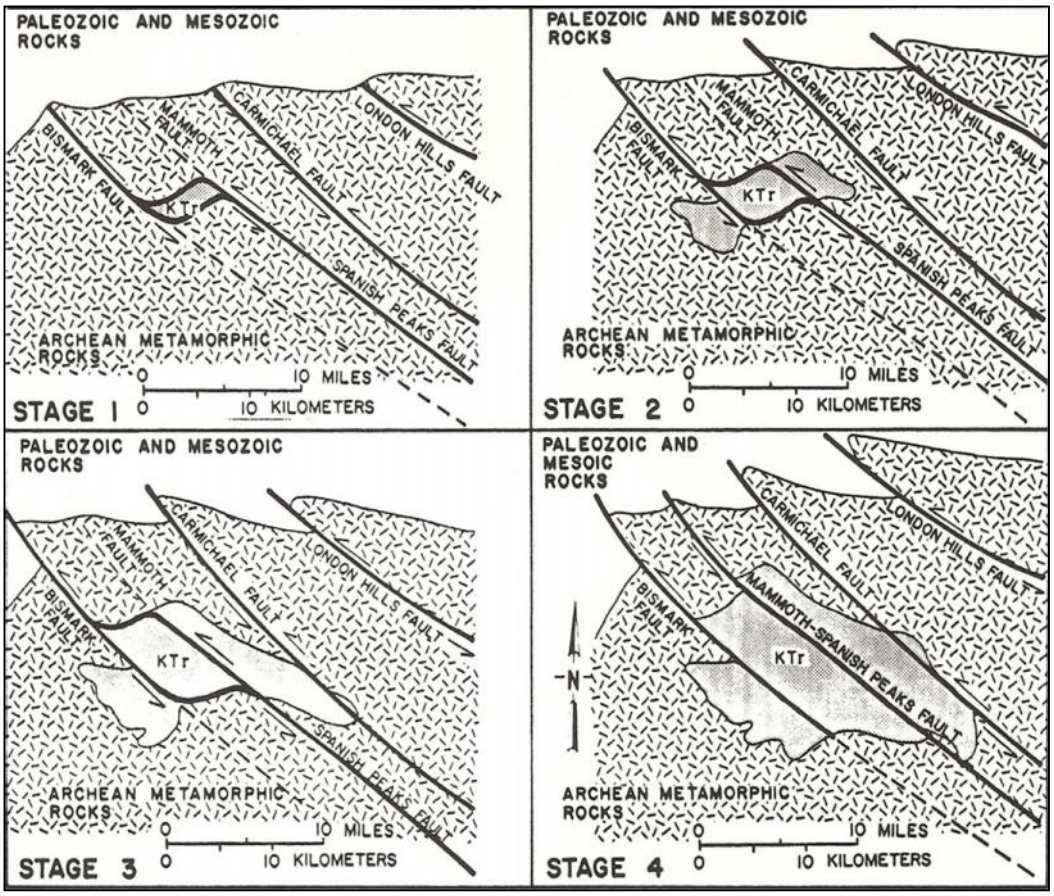

Figure 5: Fault evolution indicating emplacement of the Tobacco Root batholith (Schmidt, 1990)

A number of un-metamorphosed diabase dikes intrude Archean metamorphic rocks and show a strong alignment parallel to the northwest trending fault sets. The largest dike was intruded into the Mammoth fault zone and is roughly 300 meters wide and 6.8 km long (Schmidt and Garihan, 1986). Small branches of the Mammoth fault dikes are truncated by the Paleozoic-Archean unconformity suggesting that the dike was post Late Archean metamorphism and Pre-Paleozoic. Rubidium/Strontium age dates for the diabase dikes suggest at least two distinct periods of Middle Proterozoic dike intrusion: one between 1.45 Ga to 1.43 Ga and the other between 1.13 Ga to 1.07 Ga (Wooden et al, 1978). Dikes indicate that the faults were probably

extensional in origin and probably formed during opening of the Belt Supergroup sedimentary basin a few kilometers to the north.

Late Mesozoic to Cenozoic

The Laramide style of deformation may be found in numerous basement-cored ranges from Montana to New Mexico. During the Late Cretaceous and Paleocene in southwestern Montana active crustal shortening created oblique left-lateral slip motion on previous Proterozoic normal faults. These faults and their associated folds in the Paleozoic and Mesozoic sedimentary cover rocks are typical of the "Laramide style" of deformation in the Rocky Mountain foreland. Movement on the northwest-trending faults associated with the Tobacco Root batholith is responsible for several tens of kilometers of shortening of the foreland crust, and the inferred slip directions are consistent with a predominantly west-to-east direction of compression (Schmidt and Garihan, 1983, 1986). The northwest- trending faults that cut through the Tobacco Root batholith and Archean basement rocks comprise one of the principal deformational fabrics in the area of the batholith. The movements on the faults within the adjacent thrust belt north and west of the batholith indicate shortening suggesting the same compressional forces were responsible for the structural features both in the thrust belt and the foreland (Schmidt and Garihan, 1983, 1986). Radiometric ages of plutonic rocks in the Tobacco Root area indicate that faulting was Late Cretaceous (Vitaliano et al. 2004). Deformation progressed from west to east between Late Cretaceous and late Paleocene time (Schmidt and Garihan, 1986).

The former Laramide Rocky Mountain foreland and Cordilleran thrust belt in southwestern Montana are occupied by basin-range features associated with the

northeast part of the Basin and Range province (Reynolds, 1979; Schmidt and Garihan, 1986). The contractional Laramide features likely concentrated the basin marginal faults during later events of basin-range extension (Schmidt and Garihan, 1986). The northwest-trending faults associated with the Tobacco Root Mountains developed normal movement during the Neogene. The Neogene period of extension produced reactivation of segments of pre-existing faults, (Schmidt and Garihan, 1986).

Petrology and Lithology

The Tobacco Root batholith was emplaced into the regionally metamorphosed Archean basement rocks, which contain late Precambrian mafic dikes. Phanerozoic sedimentary rocks overlie the Precambrian rocks to the north and west and also contain Late Cretaceous intrusions. The batholith itself is a zoned pluton composed of several granitic rock types (Figure 6).

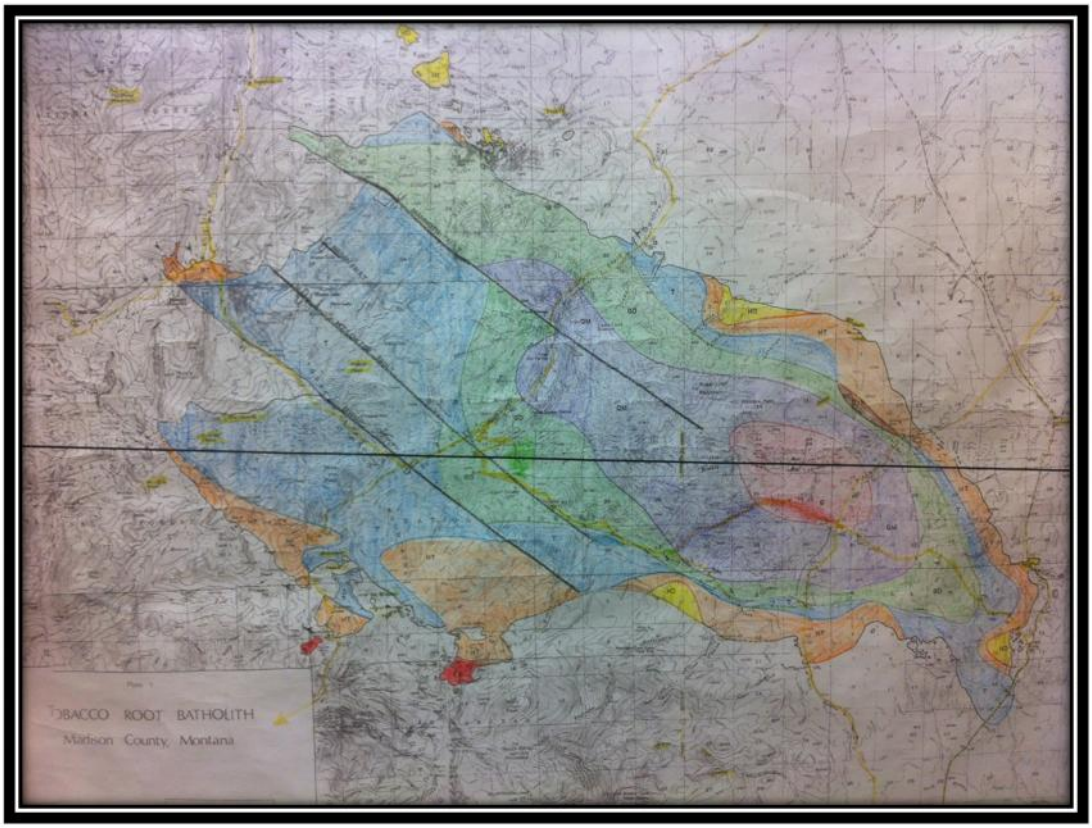

Figure 6: The zoned Tobacco Root batholith mapped by Smith (1970) comprising of hornblende diorite (yellow), hornblende tonalite (orange), tonalite (blue), hornblende granodiorite (brown), granodiorite (green), quartzmonzonite (purple), granite (red), diabase (dark red). (Smith, 1977)

Archean Rocks

The metamorphosed Archean basement rocks that surround the Tobacco Root batholith consist of many different lithologies and are structurally complex. Vitaliano et. al. (2004) identify a number of different lithologies. These are: quartzofeldspathic gneiss, hornblende gneiss, anthrophyllite-gedrite gneiss and schist, quartzite, aluminous schists, iron-formation, marble, pegmatite, orthoamphibolites, and meta-

ultramafic rocks. For the purpose of this study samples of the Archean rocks that are marginal to the batholith consist of amphibolite (orthoamphibolites), quartzofeldspathic gneiss, and hornblende gneiss. A total of 24 hand samples of these rocks were collected to determine an average density for the host rocks of 2.87 g/cm^3 for the Archean basement rocks (Theodore Bornhorst of Michigan Technological University did the density determination. A dry bulk density due to the samples being acquired above the water table was used). Calculations of rock density are discussed in Chapter III Data Collection and Reduction. In general, the strike and dip of foliation in the Archean rocks is parallel to the margins of the batholith. The strike and dip of the foliated rocks surrounding the batholith contacts, especially evident on the northern and western margins, suggests that foliation controls part of the intrusion.

Batholith Rocks

The Tobacco Root batholith is composed of felsic plutonic rocks of Late Cretaceous age. Hand samples were collected along transects over the changes in lithologies within the batholith. Based on the map by Smith (1977), the hand samples obtained in the field accurately correspond to the different rock types within the batholith. Smith's (1977) modal and chemical analyses show a gradational zoning from the outer portion of the batholith to the central region, with a change of rock type (from outer margin inward) of Hornblende Diorite, Hornblende Tonalite, Tonalite, Granodiorite, Quartzmonzonite, and Granite (Figure 6). Smith shows displacement of these lithologies by the principal faults indicating that fault movement occurred after the emplacement of the batholith. Studies of the compositional variation of K-feldspar, plagioclase, and biotite (Smith, 1970; Klusman, 1969) confirm the gradual change from the outer portion of the batholith to its core (Vitaliano, 2004). K-Ar

dating done by Vitaliano et al. (2004) determined an age of 74 to 71 Ma for the rocks of the batholith. A number of smaller silicic plutonic rock bodies are located outside the batholith to the west, suggesting that magma may have had a source from the northwest. An average density of 2.67 g/cm^3 from dry bulk density values was used in modeling the gravity field giving an average density contrast of 0.20 g/cm^3 compared to the Archean metamorphic rocks. The different granitoids obtained in the field and that correspond to the lithologies of Smith's (1977) map were also incorporated in modeling density contrasts within the batholith.

CHAPTER III

DATA COLLECTION AND REDUCTION

Introduction

The gravitational force of the earth can be used to determine information about materials within the Earth (F=mg). Gravity (g) shows minor variations on the Earth's surface due to differences in subsurface rock density. As a potential field, gravity field strength and direction are dependent on position on the Earth's surface relative to its center (Telford, et al 1990).

Data from each gravity station was obtained from the end of July to mid-August of 2011. The survey covered an area of just over 300 km^2 and four NE-SW trending transects were surveyed perpendicular to the strike of the batholith. The location of the gravity survey transects was based on geological maps produced by Smith (1977) and Vitaliano (2004).

Field Survey

The field survey was done mainly along the roadside and along hiking trails. There were a few instances where off-road and off-trail trekking was involved in order to keep along strike of a transect line. Gravity stations had a spacing of approximately 500 meters (about 0.3 miles). The total number of stations was 232, and these were reoccupied at certain points (base stations) throughout the survey for quality assurance and drift correction. Readings at gravity stations that were deemed erroneous were stricken from the data during post processing. Each transect had its own base station, and for long transects multiple base stations were used. Base stations were usually located at the center of each transect. A central base station

located at 45 46’ 15” and 111 56’ 47” just north of the survey area was established as a reference station for differential correction during post processing. To accurately measure elevation, latitude and longitude at each station, and to apply the drift correction by reoccupying each base station a Trimble GeoXH with Terrasync Global Positioning Unit (GPS) was used. The gravimeter used during this survey was a LaCoste & Romberg model G-149.

Equipment

The LaCoste & Romberg Land Gravity Meter is thermostatically controlled. Its gravity response system is a weight on the end of a horizontal beam supported by a zero-length spring. The shock eliminating springs form a floating pivot eliminating any friction in the moving system (Figure 7). In order to produce a gravity reading the gravimeter must be leveled on a concave leveling disc.

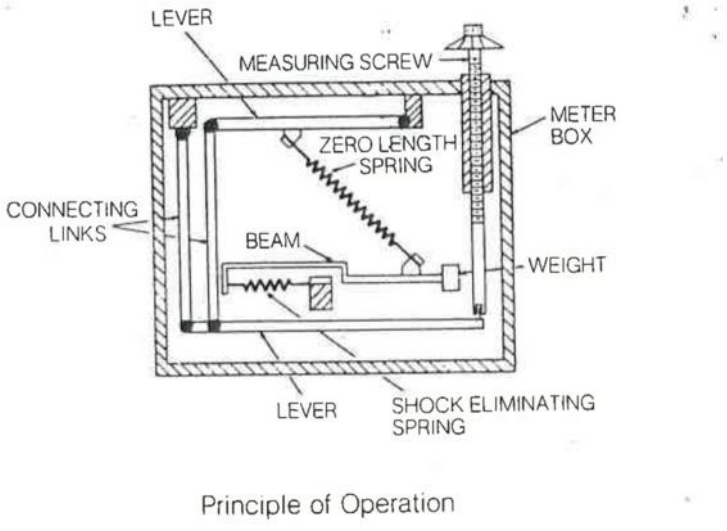

Figure 7: Principle operation schematic of the LaCoste & Romberg Land Gravity Meter.

Once the gravimeter is leveled the beam of the gravimeter is released and the measuring screw is turned until the crosshair in the viewfinder is lined up with the reading line (Figure 8). This produces a dial reading, which is converted to gravity in mGals by multiplying the interval factor by the dial reading.

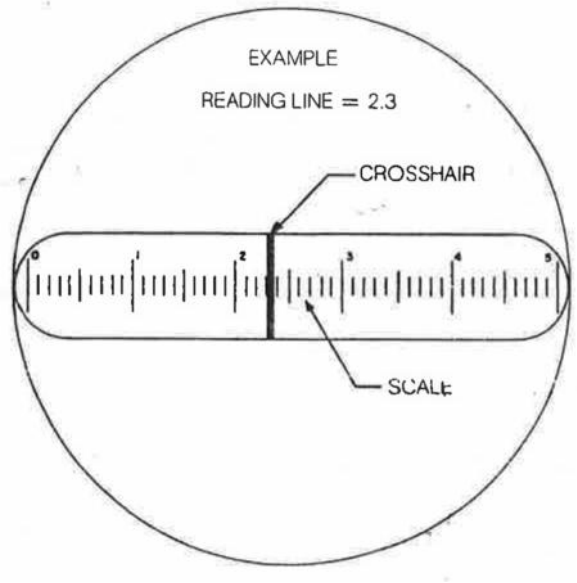

Figure 8: Schematic look through the viewfinder from the LaCoste & Romberg Land Gravity Meter.

The Trimble GeoXH with Terrasync Global Positioning Unit was used to accurately measure the elevation, latitude and longitude of each gravity station in the field. Elevations determined by Digital Elevation Models (DEM) were used in comparison with the GPS to test the accuracy of the data (Figure 9). Elevation precision averaged within 3 meters when comparing GPS to DEM (Figure 10). The GPS unit used between 4 and 12 satellites, depending on locality, simultaneously, for differential processing. Differential correction uses a ground base station that broadcasts the difference between the positions indicated by satellites relative to the position in the field. The GPS Pathfinder Office software with the Differential Correction Wizard provided by Trimble was used for differential correction during

post processing and was reduced using a standard crustal density of 2.67 g/cm^3. Reoccupied stations show the accuracy of the GPS unit to be within 0.43 meters for elevation, 0.0079 seconds latitude, and 0.0513 seconds longitude.

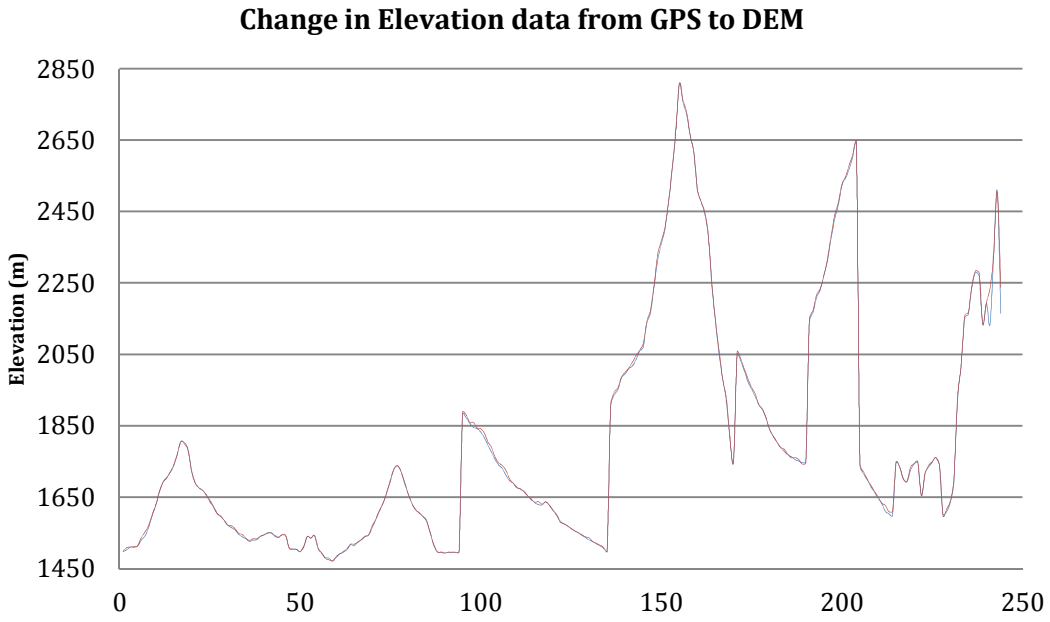

Figure 9: Difference in elevation data from DEM in red to GPS in blue.

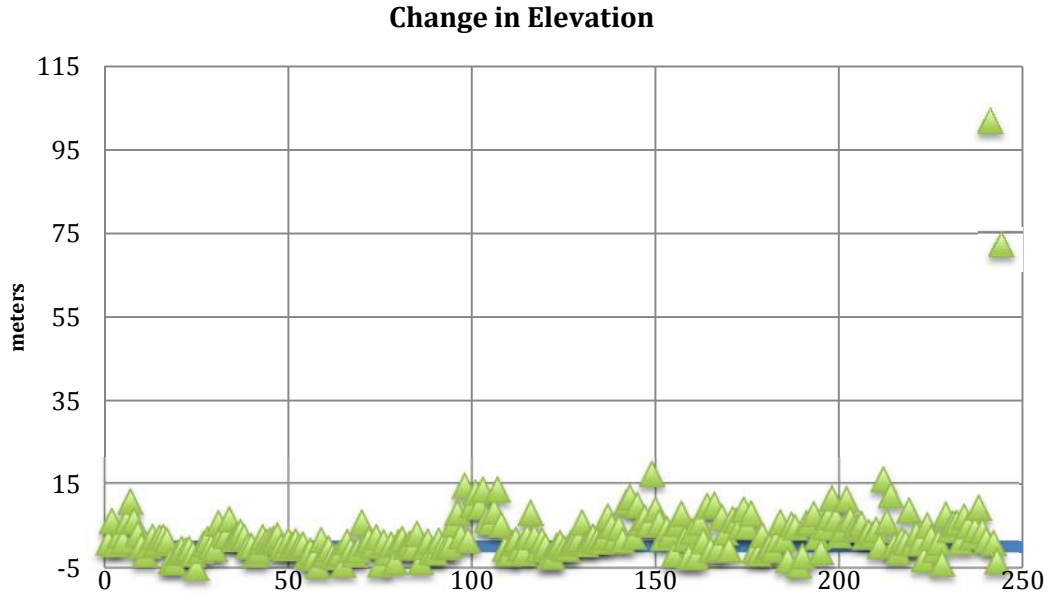

Figure 10: Comparing elevation difference from DEM to GPS.

Reduction of Field Data

Taking into account that the Earth is not a perfect homogeneous sphere, the gravitational acceleration is not constant over a multitude of gravity stations (Telford 1990). Before post processing, corrections were made for drift, latitude variation, elevation, gravitational attraction of material between the station and the sea level datum, terrain, and density.

Drift Correction

Gravimeter readings change with time as a result of elastic stretching (creep) in the spring. This creep produces an apparent change in gravity at each station. Instrumental drift can be measured by reoccupying a station (base station) at different times throughout the day (usually 2-4 hours). Once Instrumental drift measurements are calculated they are subtracted from the observed gravity measurements at each station, thus correcting for drift. Drift corrections also correct for lunar and solar tidal variations in gravity if the base station is re-occupied at 2-hour intervals or less.

Theoretical Sea Level Gravity (Normal Gravity)

To correct for latitude variations from station to station the Geodetic Reference System 1967 (GRS67) was used (equation 1)

$$g_t = 978{,}031.85(1 + 0.005278895\sin^2\phi + 0.000023462\sin^4\phi)\ \text{mGal}$$

Equation 1: where, ϕ is latitude of the observed field station. A gal (or galileo) is a unit of acceleration where the gal is defined as 1 centimeter per second squared (1 cm/s^2). The milligal (mGal) refers to one thousandth of a gal. (Lillie, 1999)

Free Air Correction

The Free Air Correction accounts for changes in station elevation. The term Free Air Correction refers to changes in elevation between gravity measured at sea level and elevation measured at a field station with no material in between. This value is given by

$$\frac{dg}{dR} \approx -0.308 \text{ mGal/m}$$

Equation 2: where, dg/dR ≈ -0.308 mGal/m, the average value for change in gravity with increasing elevation. The free air correction is then

Free Air Correction = h x (0.308 mGal/m)

Equation 3: where, h is elevation of station above a sea level datum. (Lillie, 1999)

Free Air Gravity Anomaly

The Free Air Gravity Anomaly accounts for both latitude (Theoretical Sea Level Gravity) and elevation (Free Air Correction). When subtracting the Theoretical Sea Level Gravity from the observed gravity and adding in the Free Air Correction (Equation 3), the Free Air Anomaly effectively puts the station at sea level, this requires an increase in gravity.

$$\Delta g_{faa} = g - g_{tslg} + \text{Free Air Correction}$$

Equation 4: where, g is the observed gravity, and g_{tslg} is the Theoretical Sea Level Gravity. (Lillie, 1999)

Bouguer Correction

The Bouguer Correction accounts for the gravitational attraction of material between the station and the sea level datum. This is done by assuming a slab of uniform density (2.67 g/cm^3) and an infinite horizontal extent, whose thickness is the elevation of the station (Equation 5).

$$\text{Bouguer Correction} = 2\pi\rho Gh$$

Equation 5: where, ρ is the density of the slab (2.67 g/cm^3), G is the Universal Gravity Constant of 6.67 x 10^{-11} N (m/kg^2), and h is the station elevation.

When the values of 2π and G are combined in the SI units the result yields:

$$\text{Bouguer Correction} = 0.0419\rho h$$

Simple Bouguer Gravity Anomaly

The Simple Bouguer Anomaly reduces the gravity data by subtracting the effects of an infinite flat slab of rock (between sea level and station elevation), with density ρ from the Free Air Gravity Anomaly (Equation 6).

$$\text{Simple Bouguer Anomaly} = \Delta g_{faa} - \text{Bouguer Correction}$$

Equation 6: where, Δg_{faa} is the Free Air Anomaly.

Terrain Effect

The Tobacco Root Mountains have considerable variations in elevation, and with profiles in both mountainous terrain and in valleys, a terrain correction is a necessity in order to accurately reduce the data for post processing. The Bouguer Correction does not take into consideration the presence of hills and valleys; it merely assumes an approximation to a semi-infinite horizontal slab of rock between the measuring station and sea level. A gravity measurement obtained either next to a hill or a valley requires a correction to be added to that measurement to account for the excess of mass above the station elevation, or missing mass below it. The terrain correction effectively removes the effects of the topography to fulfill the Bouguer approximation of a semi-infinite slab.

In order to make terrain corrections, manual computation may be carried out for each gravity station in the survey area. A series of 7.5' topographic maps with 1:24,000 scale of Madison County, Montana were used along with a transparent template, known as the Hammer chart (Hammer, 1939). The Hammer chart consists of a series of segmented concentric rings and is superimposed over the 7.5' topographic map to get an estimated average of the elevation for each segment. The terrain correction method works on the principle of determining the value of gravity at the center of an annulus of inner and outer radii using the equation (Reynolds, 1997) (Equation 7):

$$\delta g_{seg} = \frac{2\pi\rho G}{N} \left[r_2 - r_1 + (r_1^2 + z^2)^{\frac{1}{2}} - (r_2^2 + z^2)^{\frac{1}{2}} \right] \text{(g.u.)}$$

Equation 7: where, N is the number of segments in the ring, z is the modulus of the difference in elevation between gravity stations and mean elevation of the

segment, ρ is the Bouguer correction density (kg/m^3), r is the radius of the ring, G is the Universal Gravitational Constant of 6.67 x 10^{-11} N (m/kg^2), and g.u. refers to gravity units where g.u. = 0.1 mGal.

A table generated by Equation 7 is used to derive the terrain corrections in g.u. for each segment and summed to produce an exact calculation of the contribution of each annular ring segment correcting for each station, with each ring of the Hammer chart having a different calibration constant (Reynolds, 1997).

A digital method, implemented in the Oasis montaj Gravity & Terrain Correction software has also been applied to correct for variations in topography. The Oasis montaj Gravity and Terrain Correction system calculates the regional terrain correction from a coarse regional Digital Elevation Model (DEM) draped over a more finely sampled local DEM model that covers the survey area. This produces a regional correction grid that represents terrain corrections beyond a local correction distance (21.9 km) and can be re-used to calculate detailed corrections at each observed gravity location. The system uses the grid average elevation to compensate for terrain effects in the area past the outer (regional) correction distance.

Terrain corrections were done both manually and digitally to account for variations between gravity stations (Table 1 and Figure 11 and Figure 12) (Hammer chart and The Oasis montaj Gravity & Terrain Correction software). Terrain corrections done manually are laborious and time-consuming resulting in a fewer number of corrections made with the Hammer chart. Also, manual attempts did not extend far enough to cover all rings at all azimuths. Therefore they were incomplete, and would always give a correction less than that of Oasis. By using the Oasis montaj Gravity & Terrain Correction software, each gravity station was accounted for and compared with the stations done manually (Table 1 and Figure 11 and Figure 12).

Due to the number of gravity stations in this survey the Oasis montaj Gravity & Terrain Correction software was used. Terrain corrections in mountainous areas produced values of +10 mGals, while terrain corrections in valleys produced values of +1 mGal. The average terrain correction for the entire survey area is +3 mGals.

Station	GPS_Elevation (m)	DEM_Elevation (m)	Hammer radius (km)	OMGTC_Radius (km)	Hammer_TC (mGal)	OMGTC (mGal)	Delta (mGal)
-8	1543.22	1542.41	2.61	21.9	0.224	0.448	0.223
-5	1511.83	1511.18	2.61	21.9	0.746	0.954	0.208
-2	1502.01	1504.21	4.47	21.9	0.371	0.707	0.336
1	1498.54	1498.52	4.47	21.9	0.753	1.104	0.351
5	1513.44	1513.77	6.65	21.9	1.202	1.535	0.333
8	1563.61	1568.77	6.65	21.9	1.323	1.559	0.236
11	1664.81	1661.97	6.65	21.9	0.684	1.026	0.343
14	1719.40	1719.29	6.65	21.9	0.912	0.933	0.021
17	1805.32	1805.80	9.9	21.9	1.064	1.286	0.222
20	1723.73	1721.30	9.9	21.9	1.276	1.345	0.069
23	1670.48	1668.96	9.9	21.9	1.286	1.284	-0.002
26	1624.06	1622.88	9.9	21.9	1.483	1.595	0.112
29	1585.53	1584.64	9.9	21.9	1.773	1.549	-0.224
32	1558.92	1560.97	9.9	21.9	2.220	1.996	-0.224
35	1533.96	1534.80	9.9	21.9	0.964	1.331	0.367
39	1540.94	1540.03	6.65	21.9	0.422	1.175	0.753
43	1541.42	1542.67	6.65	21.9	0.618	1.308	0.690
46	1542.18	1542.93	4.47	21.9	0.682	1.529	0.847

Table 1: Comparison in terrain correction values from the Hammer chart and Oasis montaj Gravity & Terrain Correction (OMGTC) software. Hammer chart radii varied dependent on map space.

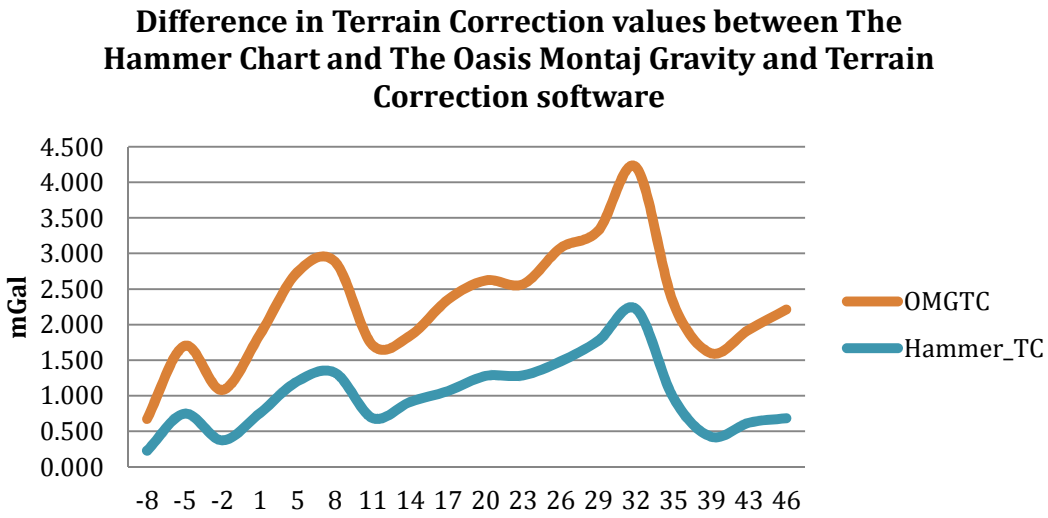

Figure 11: Linear depiction of the Hammer chart terrain corrections and the Oasis montaj Gravity & Terrain Correction software (OMGTC).

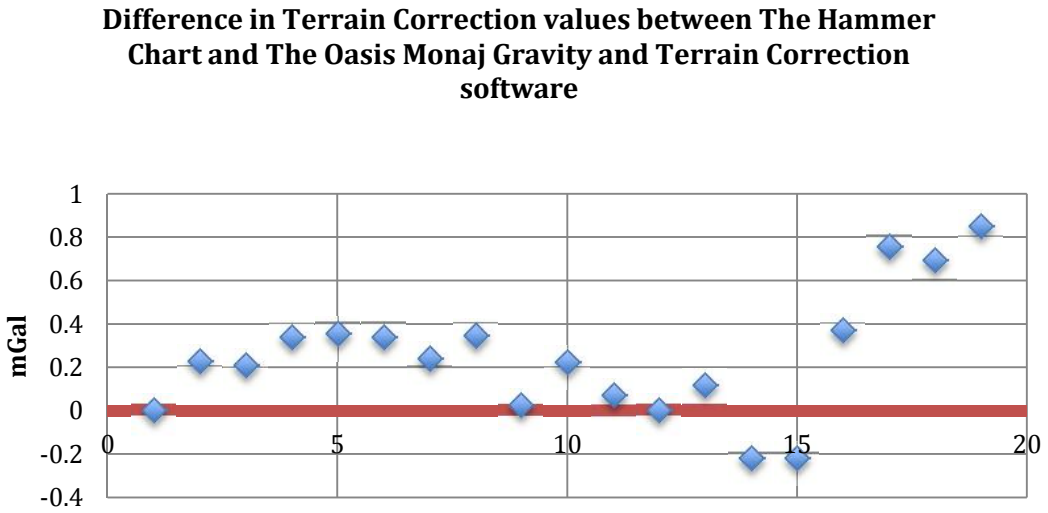

Figure 12: Scatter plot depiction in the difference in mGal from the Hammer chart terrain corrections and the Oasis montaj Gravity & Terrain Correction software (OMGTC).

Complete Bouguer Anomaly

The Terrain Correction must be added to the Simple Bouguer Anomaly to produce the Complete Bouguer Anomaly (Equation 8):

$$\Delta g_{BC} = \Delta g_{SB} + TC$$

Equation 8: where, Δg_{BC} is the Complete Bouguer Anomaly, Δg_{SB} is the Simple Bouguer Anomaly, and TC is the Terrain Correction.

Density

While density of different lithologies was not used in the basic calculations to produce the Simple Bouguer anomaly map, these measurements were necessary for the interpretation or modeling stage of this study. Density determination was performed in the laboratory and conducted by Theodore Bornhorst from Michigan Technological University (Table 2). Density analysis done for this research was from rocks collected along outcrops in the field area. Laboratory results can rarely pinpoint the true bulk density due to the samples being weathered, fragmented, dehydrated, or altered in the process of being obtained (Telford, 1990). Because the samples obtained for this project were taken above the water table the dry bulk density was used as a guide in post processing.

Analytical Number	Weight on Receipt	Dry Weight grams	Calculated on Receipt	GeoPyc 1360 Dry Bulk Density	AccuPyc 1330 Particle Density	Calculated	Calculated Saturated Bulk Density	Rock
	grams	grams	% Moisture	gm/cc	gm/cc	% Porosity	gm/cc	
Nic Mine 1	82.06	81.90	0.19	2.96	3.00	1.33	2.97	Amphibolite
Nic Mine 1A	91.25	91.11	0.15	2.97	2.99	0.67	2.98	Amphibolite
Nic Mine 2	66.82	66.73	0.13	2.69	2.69	0.00	2.69	Quartzofeldspathic Gneiss
Nic Mine 2A	62.61	62.53	0.13	2.67				Quartzofeldspathic Gneiss
Nic Mine 3	68.08	68.05	0.04	2.66	2.69	1.12	2.67	Quartzofeldspathic Gneiss
Nic Mine 3A	66.26	66.23	0.05	2.69				Quartzofeldspathic Gneiss
Nic Mine 4	71.21	71.13	0.11	2.65	2.68	1.12	2.66	Quartzofeldspathic Gneiss
Nic Mine 5	60.30	60.21	0.15	2.66	2.68	0.75	2.67	Granitoid (Hornblend Tonalite/Tonalite)
Nic Mine 5A	61.46	61.38	0.13	2.65				Granitoid (Hornblend Tonalite/Tonalite)
Nic Mine 6	77.84	77.84	0.00	3.11	3.14	0.96	3.12	Hornfelds
Nic Mine 7	55.53	55.43	0.18	2.70	2.75	1.82	2.72	Hornblend Gneiss
SE1	65.37	65.30	0.11	2.95	2.97	0.67	2.96	Amphibolite
SE1A	63.29	63.21	0.13	2.96				Amphibolite
SE2	58.63	58.59	0.07	2.75	2.76	0.36	2.75	Granitoid (Tonalite)
SE2A	66.03	65.98	0.08	2.73				Granitoid (Tonalite)
SE3	70.01	69.93	0.11	2.96	3.00	1.33	2.97	Amphibolite
SE3A	69.90	69.81	0.13	2.96				Amphibolite
SE4	49.10	49.04	0.12	3.04	3.03	-0.33	3.04	Amphibolite
SE4A	44.04	43.92	0.27	2.87				Amphibolite
SE5	72.14	72.10	0.06	2.88	2.92	1.37	2.89	Hornblend Gneiss
SE6	66.11	66.05	0.09	2.64	2.67	1.12	2.65	Granitoid (Granite)
287	68.63	68.51	0.17	2.70	2.72	0.74	2.71	Granitoid (Tonalite)
287A	69.43	69.34	0.13	2.72				Granitoid (Tonalite)
287-2	68.14	67.99	0.22	2.98	2.99	0.33	2.98	Amphibolite
287-3	67.31	67.15	0.24	2.78				Hornblend Gneiss
287-4	34.39	34.36	0.09	2.74	3.09	11.33	2.85	Amphibolite
SW11	75.17	75.11	0.08	2.97	2.98	0.34	2.97	Amphibolite
SW11A	73.43	73.38	0.07	2.98				Amphibolite
SW11-2	66.01	65.93	0.12	2.62	2.66	1.50	2.64	Quartzofeldspathic Gneiss
SW11-3	58.37	58.31	0.10	2.83	2.83	0.00	2.83	Amphibolite
22-1	60.92	60.84	0.13	2.68	2.77	3.25	2.71	Granitoid (Tonalite)
22-2	73.06	73.01	0.07	2.58				Granitoid (Granodiorite)
22-2A	71.91	71.82	0.13	2.60				Granitoid (Granodiorite)
22-2B	74.75	74.62	0.17	2.60	2.64	1.52	2.62	Granitoid (Granodiorite)
22-3	79.42	79.34	0.10	2.63				Granitoid (Quartz Monzonite)
22-3A	74.97	74.88	0.12	2.61	2.69	2.97	2.64	Granitoid (Quartz Monzonite)
21-4	62.81	62.79	0.03	2.66	2.70	1.48	2.67	Granitoid (Quartz Monzonite)
21-4A	67.26	67.25	0.01	2.62	2.70	2.96	2.65	Granitoid (Quartz Monzonite)

Table 2: Density determination of samples collected in the Archean Basement and Tobacco Root batholith of the Tobacco Root Mountains. Averages of 2.87 g/cm^3 for Archean basement rock and 2.67 g/cm^3 for batholitic rocks were determined using the Dry Bulk Density values.

A total of 24 hand samples of these rocks were collected to determine an average density 2.87 g/cm^3 for the Archean basement host rocks. An average density of 2.67 g/cm^3 from dry bulk density values of the granitic batholith rocks was used in modeling the gravity field, giving an average density contrast of 0.20 g/cm^3 compared to the Archean metamorphic rocks.

Error Analysis

Before conducting a gravity survey it is important to know and understand the errors associated in data collection and post processing. Extreme care was taken to avoid any error that can significantly affect the final outcome of the gravity data for reduction and post processing.

During the data collection portion of the survey error can first arise from the leveling of the gravimeter. If the leveling of the gravimeter is done incorrectly an erroneous reading will result. Any departure from level will result in a decreased reading. Also, if the gravimeter is not steady during the nulling or is subjected to drastic motion, damage to the internal spring can occur and result in measurement error.

The model G-149 Lacoste & Romberg gravimeter used in the gravity survey has a dial turn counter reading with a least count of 0.01 turns (0.01 dial units). A calibration table for the gravimeter was used to convert the counter readings into mGal (Provided by the G-149 Lacoste & Romberg gravimeter manual). For this survey The Lacoste & Romberg G-149 instruction manual provides a tabled interval factor value of 1.04805 mGal/dial unit for the range of field readings encountered and from this an estimation of the fundamental error in the gravity readings can be calculated (Equation 9).

0.01 (dial units) x 1.04805 mGal/dial unit = 0.0104805 mGal.

Equation 9: An error analysis of the G-149 Lacoste & Romberg gravimeter.

In general, this results in an estimated error of about 0.01mGals per reading.

The accuracy of the Trimble GeoXH with Terrasync Global Positioning Unit is determined by the sum of several sources of error. The contribution of each source varies depending on atmospheric and equipment conditions. Applying rigorous data collection techniques to equipment setup minimizes errors by obtaining satellite lock. Source of error include, obstruction, multipath, clock errors, ionospheric delay, and atmospheric delay. Obstruction refers to any object in the path of the signal, for instance, under a tree or in a canyon as opposed to an open field where signal is best. Multipath error occurs when the GPS signal is reflected off an object, such as a canyon wall, before it reaches the GPS antenna. Clock errors refer to the clocks in each satellite, which are subject to relativistic effects. Ionospheric delay is caused by the conductive plasma of the ionosphere. Atmospheric delay occurs when GPS signal (radio wave) is slowed by water droplets in the atmosphere (water has a high dielectric constant, which slows radio waves). Differential correction (drift correction) removes most of these errors in Global Navigation Satellite Systems (GNSS) data caused by the above factors. It improves the accuracy of GNSS positions depending on the receiver quality and data collection (time) technique used.

CHAPTER IV

RESIDUAL GRAVITY ANOMALY

Introduction

In order to make density models that are compatible with the gravity field due entirely to the batholith exclusive of any "deeper" structures below, the regional trend of the Bouguer anomaly must be subtracted from the complete Bouguer anomaly. The result is termed the residual gravity anomaly.

Simple Bouguer Anomaly Map

The Simple Bouguer Anomaly map is a map that corrects the free air anomaly for the mass of rock that exists between the station elevation and the spheroid (Figure 13). This map was produced from reduced data, with all corrections discussed in Chapter III (Data Collection and Reduction), using a standard crustal density of 2.67 g/cm^3. The anomaly is produced by variations of density in the subsurface. Each transect in the survey, indicated by white hollow circles, was taken either along rivers, creeks, or roadsides (Figure 13). The anomaly shown in this map trends NW-SE and has its lowest value (-243 mGal) in the center portion of the map (45°34', -111°55'). Steep gradients are evident near Pony and Mill Creek, north and south of the anomaly, respectively. Steep gradients can also be found just east of Highway 287, southwest of Norris, and along the South Boulder River (Figure 13). Gravitational highs unrelated to the batholith can be found outside the anomaly, as for example in the northern portion of the map near the town of Harrison. These anomalies are presumably related to basement rock density changes.

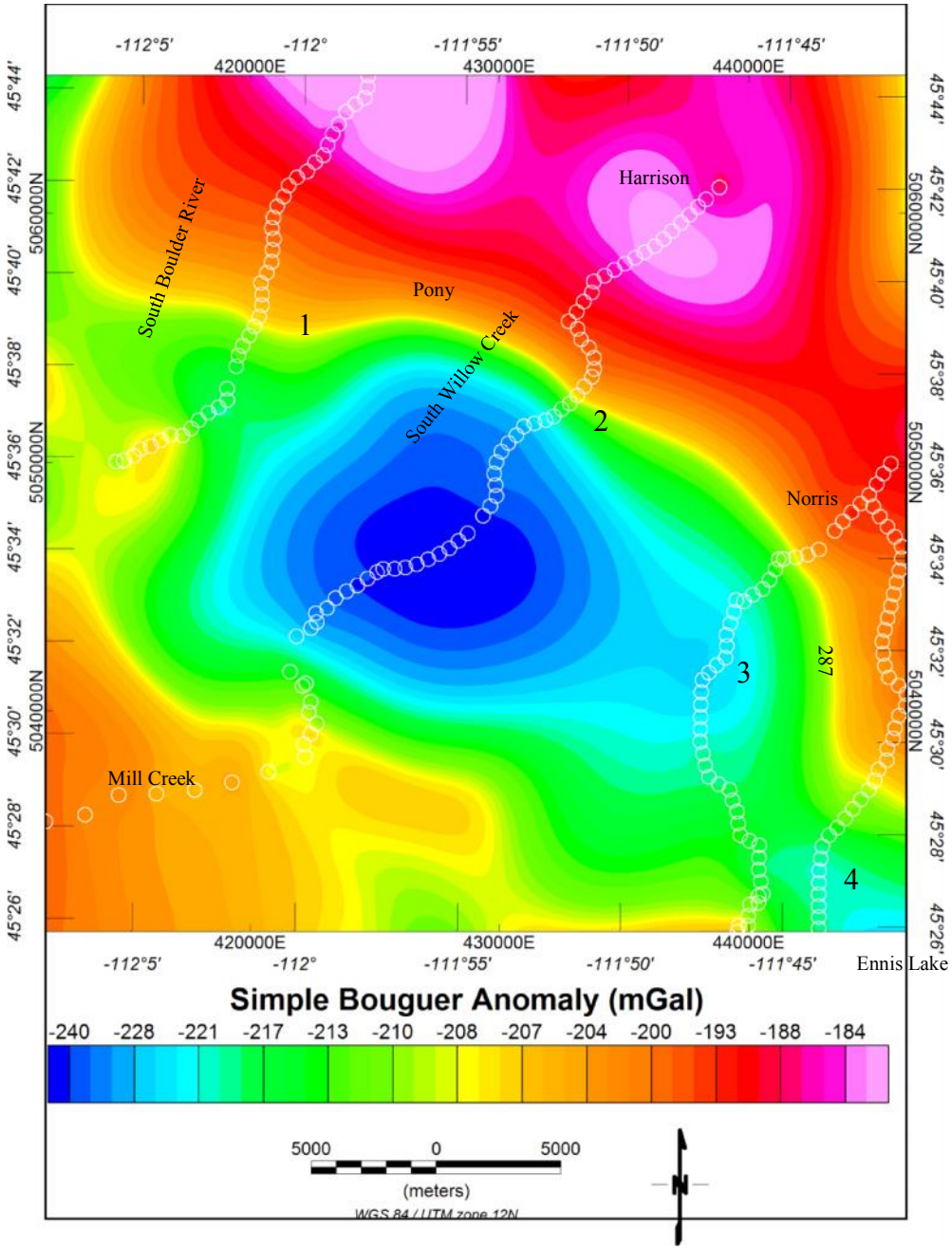

Figure 13: A Simple Bouguer Anomaly map of the Tobacco Root Mountains. White circles represent the observed gravity stations occupied in the field along transects. Gravity anomaly trends NW-SE with a gravitational acceleration low of -243 mGal.

Complete Bouguer Anomaly Map

The Complete Bouguer Anomaly map (Figure 14) corrects the Bouguer anomaly for topography in the vicinity of the observation points. This map is significantly different from the Simple Bouguer Anomaly map. However, when the terrain correction is applied there is some change to the anomaly. For example, it changes the gravity minimum by 9 mGal (from-243 to-234). The terrain correction also slightly widens the spacing between gravity contours. This is most evident in the SE portion of the map near Ennis Lake and McAllister, in the northern portion of the map near Harrison, and in the northern portion of the South Boulder River.

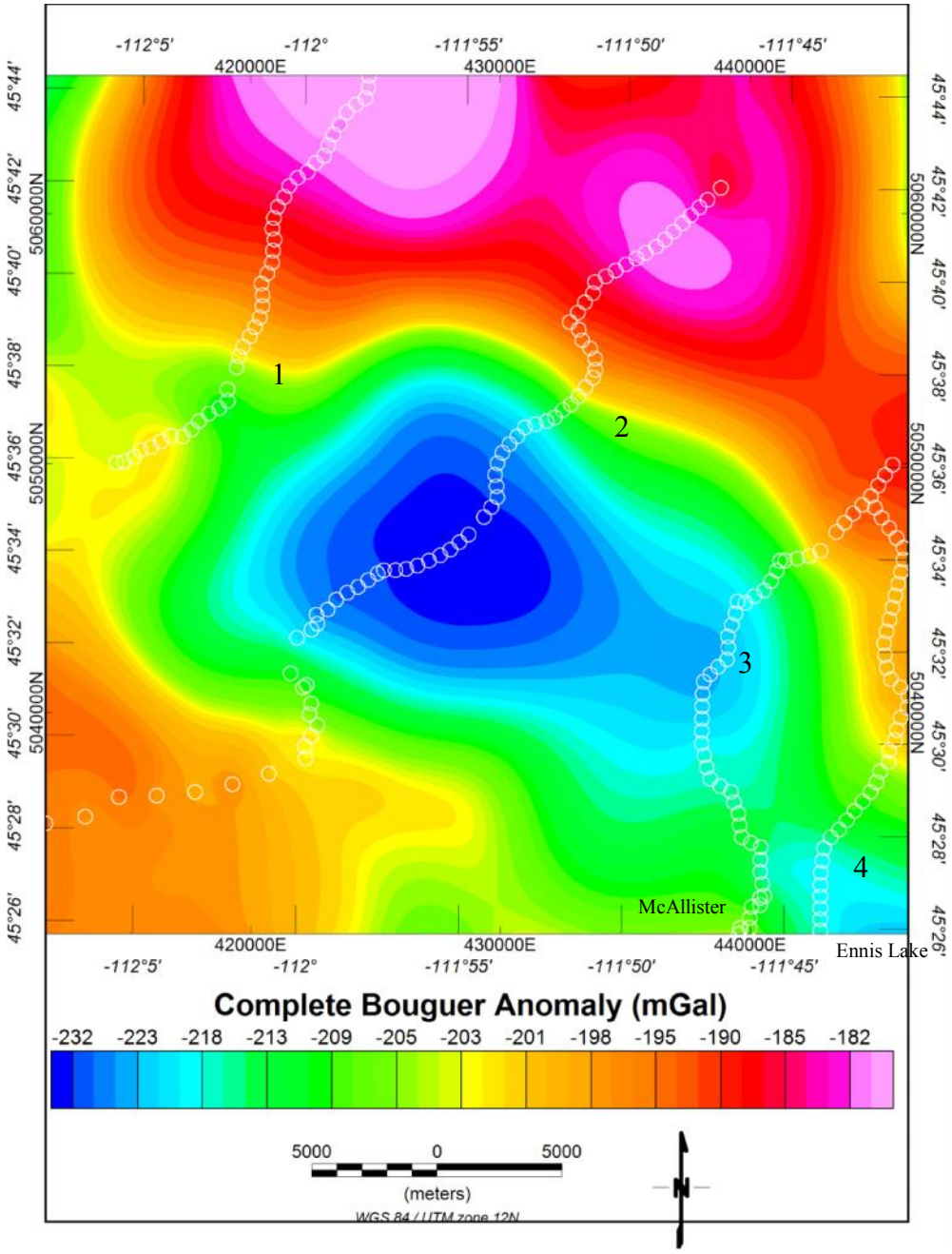

Figure 14: The Complete Bouguer Anomaly map of the Tobacco Root Mountains.

Regional and Residual Gravity Data and Map

Determining the residual gravity entails subtracting the regional gravity from the complete Bouguer anomaly, thereby isolating the anomaly from regional trends that usually have a deeper source than that of the residual anomaly. A larger scale Bouguer gravity map (Bonini, Smith and Hughes, 1973) was used to produce the residual gravity map. A regional profile (Figure 15) was drawn SW-NE, perpendicular to the strike of the Tobacco Root batholith and across the most negative part of the Complete Bouguer Anomaly.

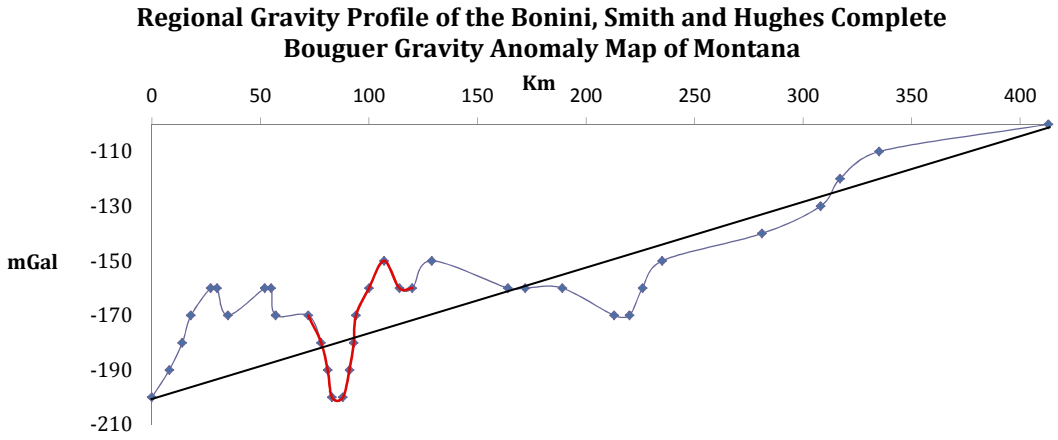

Figure 15: A regional gravity profile across the entire state of Montana SW-NE perpendicular to strike of the Tobacco Root batholith. The red line superimposed over the blue line depicts the Tobacco Root Mountain region with gravity low at -200 mGal.

The residual gravity profile (Figure 16) was computed using Equation 10, which assumes a linear regional gradient across this part of Montana. It would also have been possible to fit a sin curve or other function to determine the residual.

However, a linear function was assumed to be adequate for this study.

Residual = CBAi - (slope of trend x D) + CBAf

Equation 10: Where, CBA is the Complete Bouguer Anomaly, and D is distance.

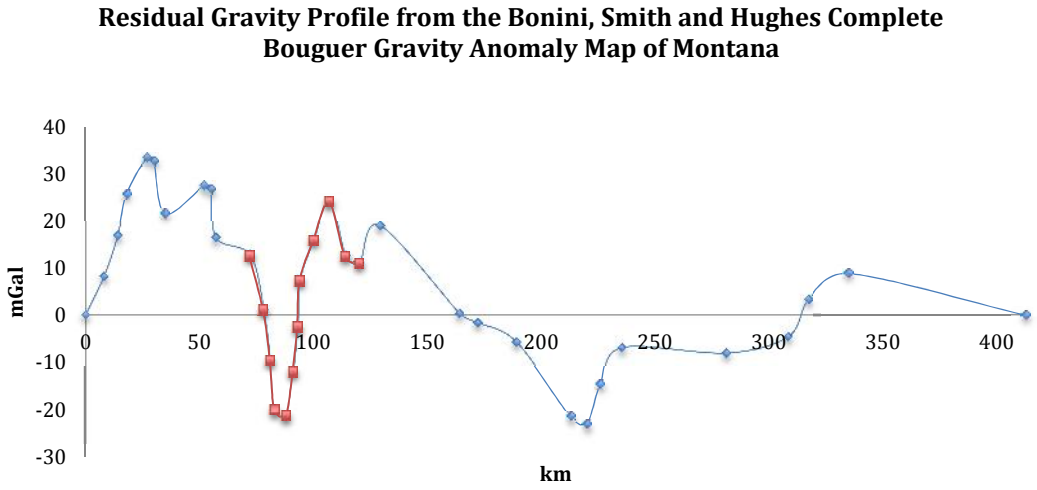

Figure 16: A residual gravity profile across the entire state of Montana SW-NE perpendicular to strike of the Tobacco Root batholith. The red line superimposed over the blue line depicts the Tobacco Root Mountain region with gravity low at -21 mGal.

Although the regional profile crosses the batholith perpendicular to strike in only one place the profile was used to reduce the gravity of the entire Complete Bouguer Anomaly according to Equation 4.1. This was justified because the regional gravity does not vary significantly perpendicular to strike in the vicinity of the batholith. Residual calculations were done to all four SW-NE trending transects to produce a residual gravity map of the Tobacco Root area (Figure 17). The Residual Gravity map isolates the gravity anomaly in the center portion of the map with a

gravity low of-44 mGal. The NW-SE trending anomaly is presumably related only to the Tobacco Root batholith and its host rocks. It has a NW-SE extent of approximately 31 km and a SW-NE extent of 20.5 km. The boundaries of the batholith are based on contact boundaries observed in the field and also by the steepness of the gravity gradients at those boundaries.

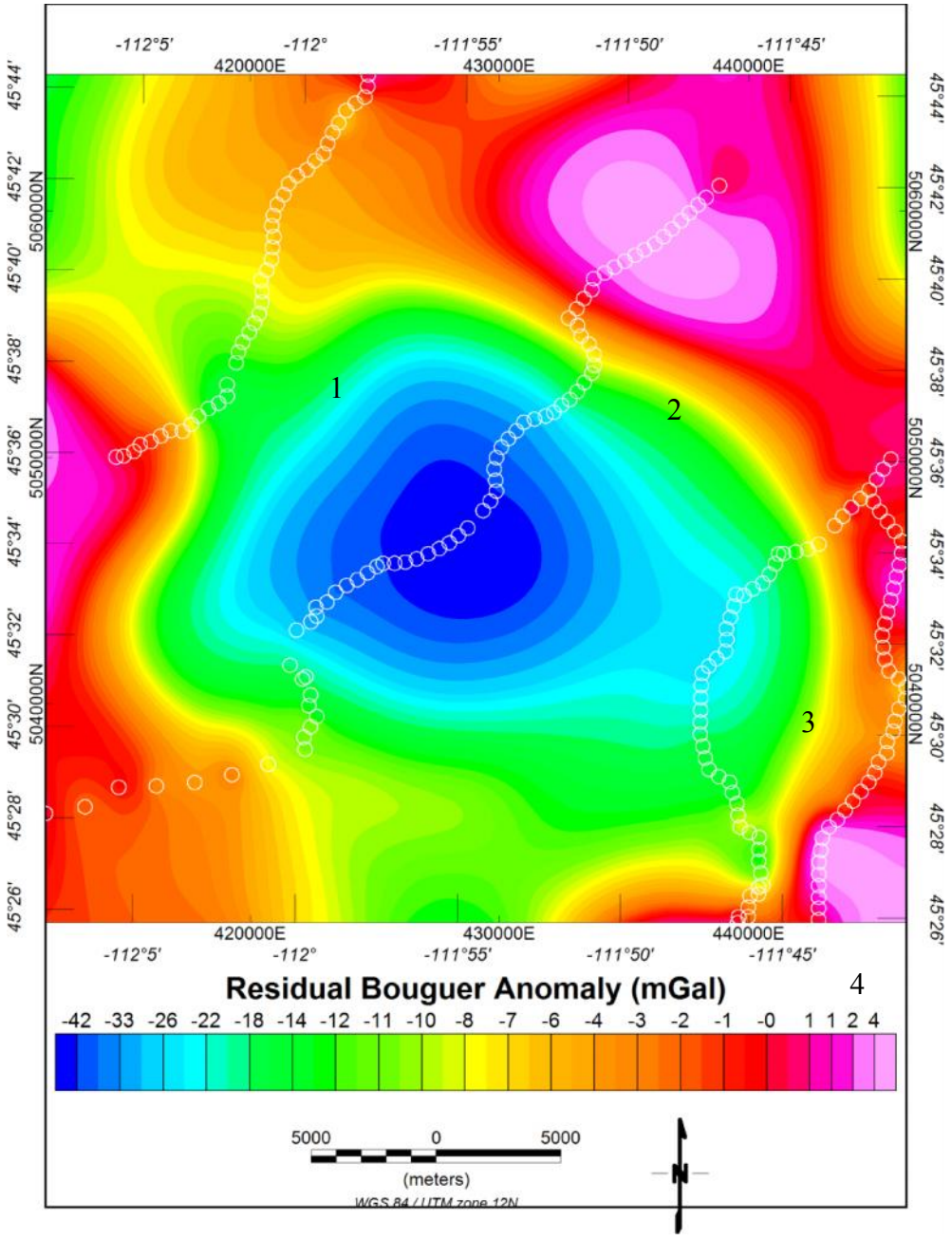

Figure 17: Residual Gravity Map of the Tobacco Root area depicting a Gravity low of -44 mGal in the center of the surveyed area. Hollowed white circles represent the observed gravity stations recorded in the field. The density contrast and gravity low are most likely due to the density of the batholith, which is not homogenous but is zoned with density variations.

CHAPTER V

INTERPRETATION

Introduction to Gravity Profiles

Forward modeling is an essential step in gravity interpretations. The forward models, were produced from the reduced data for the four different transects. Forward modeling involves calculating the gravity field from an assigned distribution of density and comparing the calculated field with the observed residual gravity, then adjusting the subsurface model and recalculating in an iterative manner. The end result is a determination of the shape and extent of the geological feature that provides the best fit to the observed gravity. However, such a model is not unique, as a great number of models may fit the same data (Appendix A). Convergence to a smaller range of models is possible if some boundaries and densities can be constrained by field mapping of surface contacts, by density measurements of samples, and by depths of lithology change from borehole data.

Gravity Profiles were produced using the Gravity and Magnetic Modeling software (GM-SYS). GM-SYS is a program used for calculating the gravitational (and magnetic) response from a geologic model. It allows the user to create and manipulate the density models to fit the observed gravity data, assuming either 2-D or 2.5-D geometries. The 2.5-D capability of the program was used to limit strike length differently in either direction. It should be noted that an infinite number of models can be manipulated to fit the observed gravity data. However, what was done for this research was to fit the observed gravity data with what is known about the structure and density of the batholith and the host rocks. Density for each lithologic units of the models is based on saturated bulk densities of rocks collected in the field and

structural data from Vitaliano and Cordura 1979.

The gravity models are controlled by density variations in subsurface materials. For modelling of gravity profiles, the program calculates the gravity field for an assumed subsurface structure, array of rock types of a given density, and compares the calculated gravity profile with the observed residual gravity profile. Systematic changes are made in the subsurface geometry consistent with known surface geology and rock density until a best fit is obtained between calculated and observed gravity for each profile. The density values were determined by direct measurement of samples from the batholith, and from the host rocks surrounding the batholith, generally Archean basement. The density values used in the models are compatible with the measured densities, and surface boundaries were placed at observed contacts between rock types, most notably that between the batholith and metamorphic basement. The surface geometry of the batholith was estimated based on the maps and literature produced from Schmidt (1979), Vitaliano et al (1979), and Smith (1977). It is important to consider all types of variables when inputting the data to produce the gravity profile. The main variables are density, subsurface geometry and extent (or depth). Density contrasts have a major influence on gravity and will change the magnitude of the observed gravity, leading to different depth estimates. The vertical extent of the batholith in the basement rocks and the dips between the contacts of the batholith and the basement rocks will influence the magnitude of the observed gravity.

By using known structural data and densities from rocks acquired in the field a number of basic models were generated in order to get an approximation of how the observed gravity will be influenced by shape and density contrasts. Multiple models of each profile were generated in order to analyze the range of possible or reasonable

models (Appendix A).

Each profile was, first, produced with a homogeneous batholith having a density of 2.67 g/cm^3 and a basement (Archean rocks) having a density of 2.87 g/cm^3 (Appendix A). Using these densities and known surface geometry as a template for each profile allowed for the incorporation of the different lithologies within the batholith. Once the approximate geometry and densities of each lithology within the batholith were established, the NW trending faults were incorporated into the profiles where transects were perpendicular to the strike of the faults. As seen by comparing Figure 19b and Figure 19 (Appendix A and Figure 19, respectively), the incorporation of the faults did not greatly change the fit to the observed gravity. However, the fit to the observed gravity did have an in influence when the different granitic densities were incorporated. The discussion below is based on the best representation of the gravity data with known geometry and obtained densities.

Westernmost Transect

Figure 18 is a profile of the west most transect from SW-NE. It depicts a calculated residual gravity low of -15 mGal and an incorporated zoned batholith with faults that cut through the batholith. The batholith consists of hornblende tonalite (orange) with a density of 2.72 g/cm^3, tonalite (blue) with density of 2.71 g/cm^3 and granodiorite (green) with density of 2.68 g/cm^3. The faults that are presented in the profile, starting from the SW are; the Bismark, Holowtop, Mason, Mammoth and the Carmichael faults. The horizontal SW-NE extent of the batholith is 16.9 km in the subsurface with a maximum depth of 6.5 km. The surrounding Archean basement rocks (maroon) have an average density of 2.87 g/cm^3. The near surface feature located on the SW portion of the profile is hornblende gneiss and granulite, mapped

by Vitaliano (1979), and was assigned a density value of 3.1 g/cm^3. The features located in the NE portion of the profile are a sill (red) and limestone (purple), assigned density values of 3.0 g/cm^3 and 2.4 g/cm^3, respectively.

Based on this profile and the residual gravity map (Figure 17) the batholith is inferred to extend northwestward in the subsurface for just over 10 km from where it is outcrops along the first transect. This inferred extension may indicate that the batholith was intruded laterally from the northwest, as originally suggested bu Burfeind (1967).

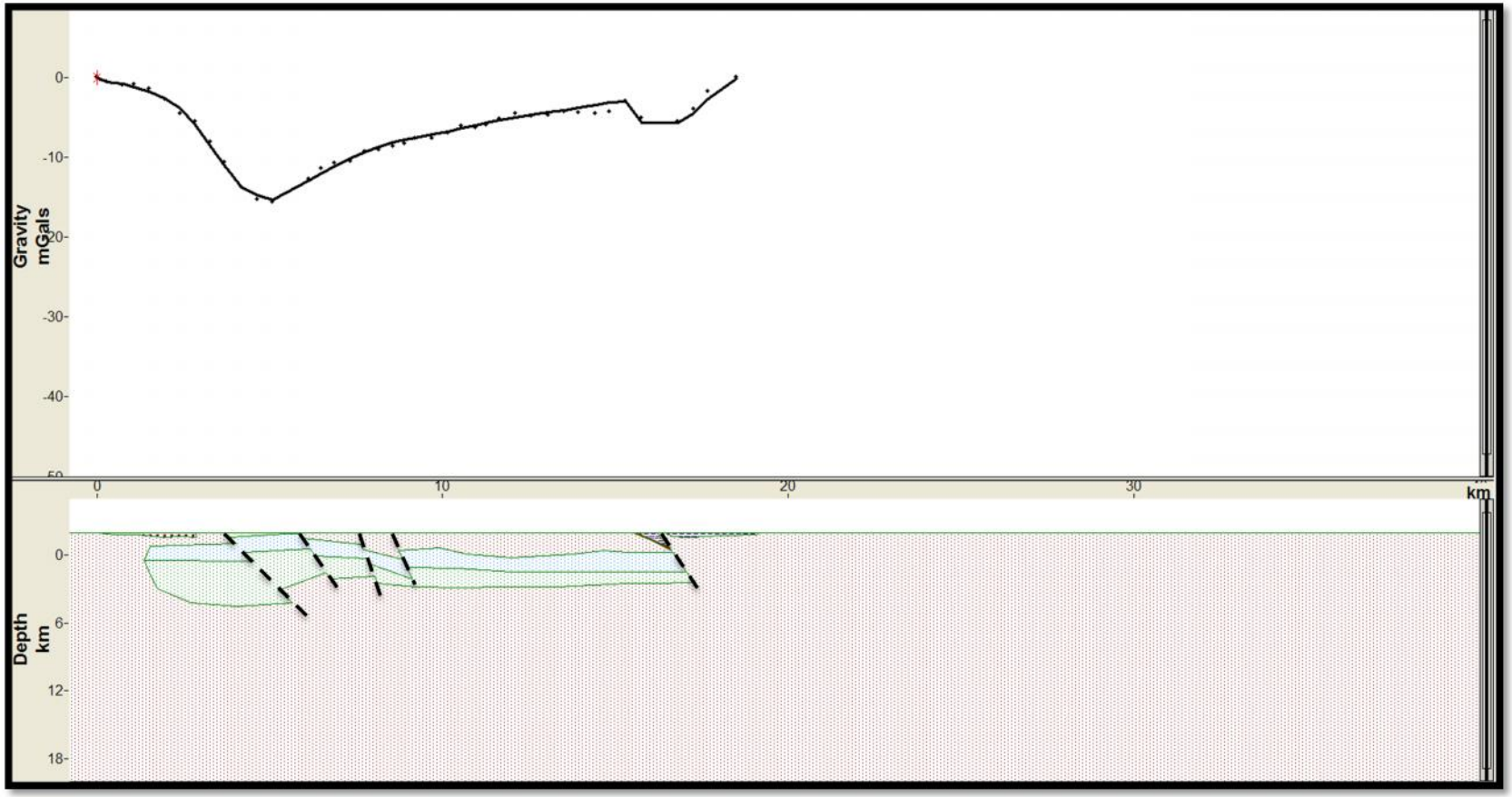

Figure 18: The westernmost profile and model from SW-NE.

West-Central Transect

Figure 19 is the profile of transect 2 extending over the center of the batholith from SW-NE. This profile shows a calculated residual gravity low of -44 mGal, the largest negative anomaly of all of the four transects. The horizontal extent of the batholith is 15.3 km and maximum depth is 20 km. The zoned batholith with incorporated faults consists of tonalite (blue) with a density of 2.71 g/cm^3, granodiorite (green) with a density of 2.68 g/cm^3, quartzmonzonite with a density of 2.675 g/cm^3, granite with a density of 2.67 g/cm^3. The surrounding Archean basement rocks (maroon) have an average density of 2.87 g/cm^3. The features located on the SW and NE portion of the profile, near the surface, are alluvium (yellow) with a density of 2.30 g/cm^3.

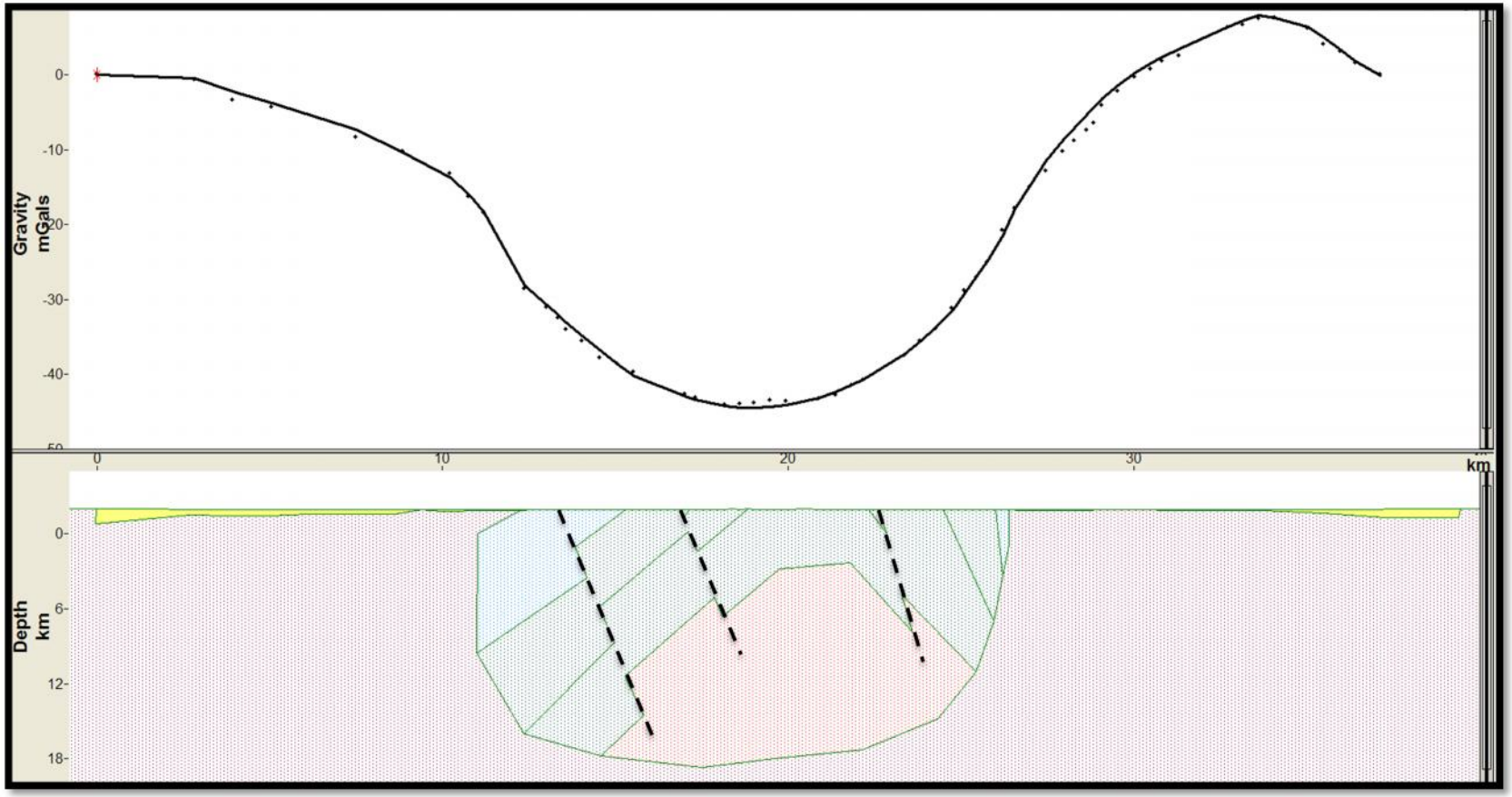

Figure 19: The west central profile and model from SW-NE.

East-Central Transect

Figure 20 is of the third transect and extends from SW-NE. This profile has a calculated residual gravity low of -25 mGal over this narrow portion of the batholith. The zoned batholith consists of hornblende tonalite (orange) with a density of 2.72 g/cm^3, tonalite (blue) with a density of 2.71 g/cm^3, granodiorite (green) with a density of 2.68 g/cm^3, quartzmonzonite with a density of 2.675 g/cm^3, and granite (red) with a density of 2.67 g/cm^3. The batholith is 9.4 km wide and has a maximum modeled depth of 12 km.. The surrounding Archean basement rocks (maroon) have an average density of 2.87 g/cm^3. The features located on the SW and NE portion of the profile near the surface are alluvium (yellow) with a density of 2.30 g/cm^3.

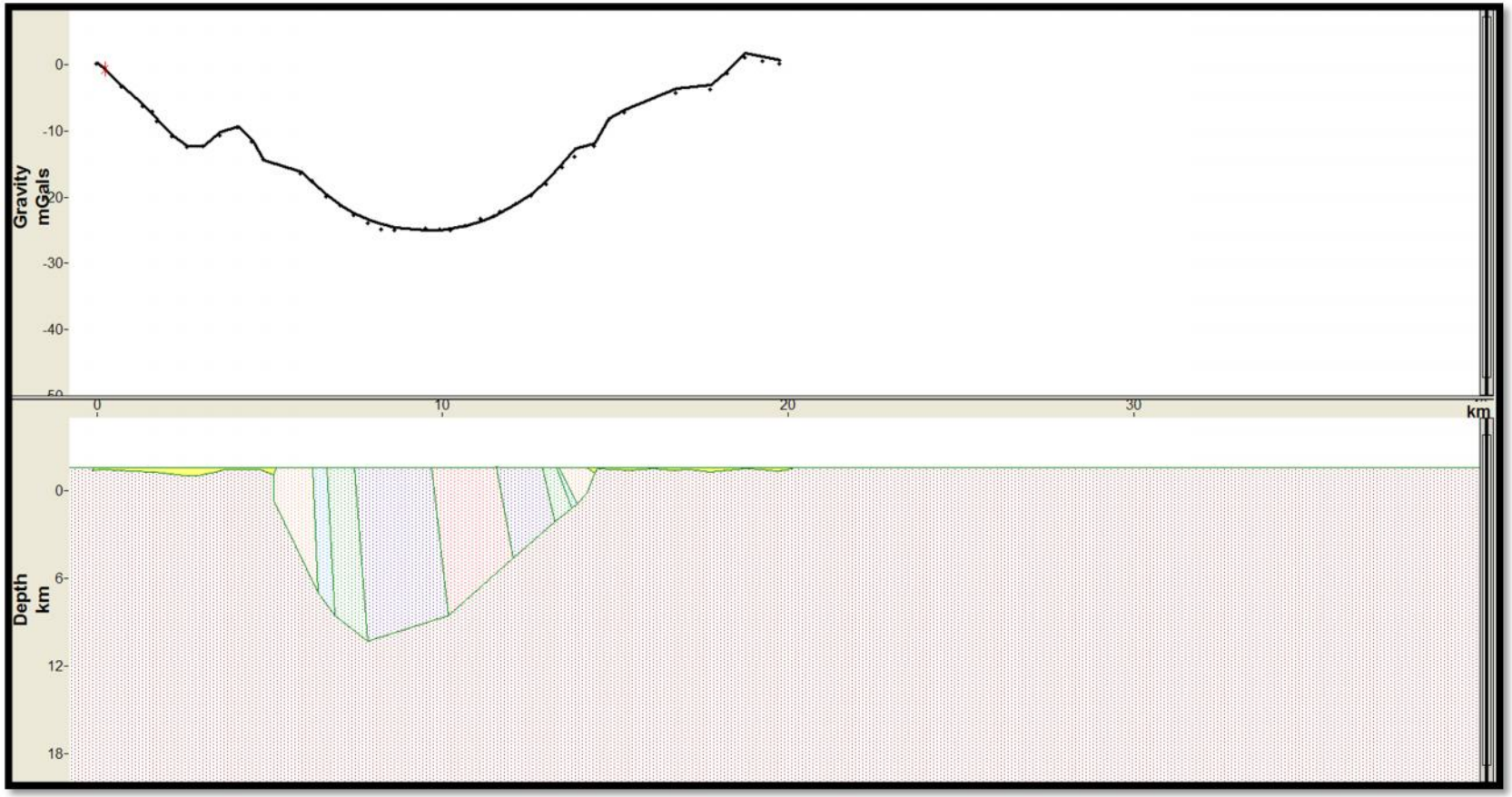

Figure 20: The east central profile and model from SW-NE.

Easternmost Transect

Figure 21 is the easternmost profile located along the southeastern-most end of the batholith. Except for 4 stations in the middle of the profile it crosses metamorphic basement rocks. The gravity low is -4 mGal. The zoned batholith as modeled here consists of tonalite (blue) with a density of 2.71 g/cm^3, and hornblende tonalite (orange) with a density of 2.72 g/cm^3. The batholith is 8.6 km wide in the subsurface and has a maximum depth of 3 km. The surrounding Archean basement rocks (maroon) have a density of 2.87 g/cm^3. The features located on the SW and NE portion of the profile near the surface are alluvium (yellow) with a density of 2.30 g/cm^3.

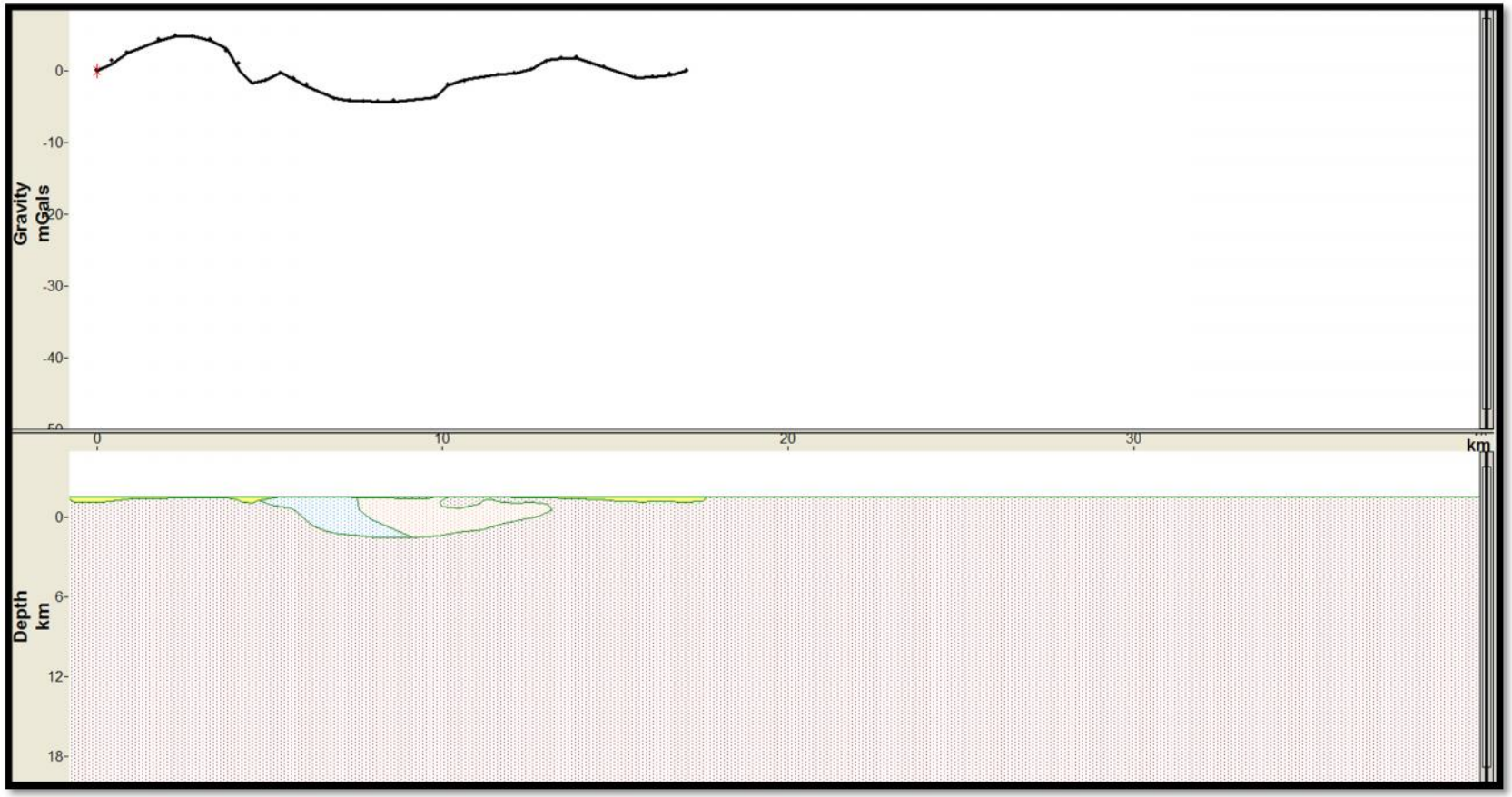

Figure 21: The easternmost profile and model from SW-NE.

Residual Gravity Map

When looking at the residual gravity map with the outline of the batholith overlaid (Figure 22), the overall geometry of the anomalous feature and the outline of the batholith correspond fairly well. It is reasonable to assume that the anomalous feature, indicated in blue with residual gravity low ranging from -44 mGals to 20 mGals, is the result of the Tobacco Root batholith.

It is important to note the moderate gravity low values depicted in green on the map. These (moderately) low values found in the southern portion and northwestern portion of the map are probably related to subsurface plutonic (ganitic) rocks. The anomalous feature found in the south center portion of the map (west of McAllister) may be a small pluton south of the Tobacco Root batholith. This corresponds very closely in proximity to a small pluton found on the map produced by Vitaliano et al (1979). The anomalous feature in the northwestern portion (Jefferson River area) of the map could possibly be an extension of the Tobacco Root batholith in the subsurface.

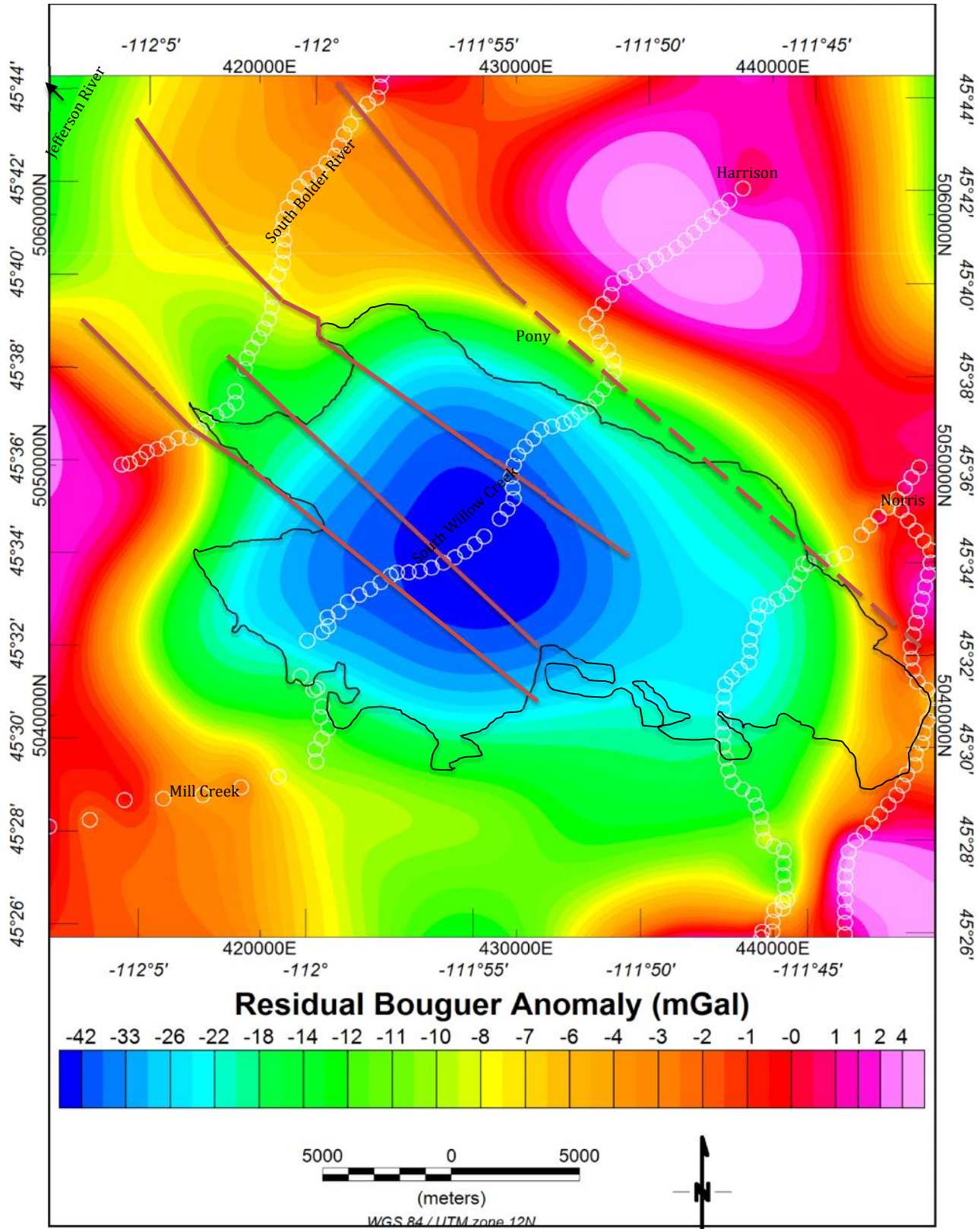

Figure 22: Residual Gravity Map of the Tobacco Root area with an outline of the batholith overlaid

CHAPTER VI

CONCLUSION

The gravitational method used during this research provided a better understanding of the subsurface configuration and depth to the base of the Tobacco Root batholith. The outcome from the primary objective is a result of images produced from reduced observed gravity data gathered in the field. The lateral extent of the batholith in the subsurface is fairly well defined on the simple Bouguer anomaly map, complete Bouguer anomaly map, and residual anomaly map.

The superimposed residual Bouguer anomaly map (Figure 22) shows gravity low in the center portion of the map. This anomalous feature represents the mass of the Tobacco Root batholith extending to its greatest depth (20 km) in the subsurface. Another gravity low to the northwest, near the Jefferson River, suggests either an extension of the pluton to the northwest or a portion of siliceous plutonic rock separated in the subsurface. This anomalous extension may indicate a northwest source of magma, presumably from the larger Boulder batholith. The major NW-trending faults in the Tobacco Root area do not have a great enough influence on the gravity data to make any notable refinement of the interpretive models. Although the NW trending faults were probably the cause and controls for the batholith emplacement during the Late Cretaceous, there is not enough lateral variation in density contrast within the batholith for the faults to have a significant effect on the gravity field.

The gravity models produced by the GM-SYS software program of the four SW-NE trending transects allows a reasonable interpretation of the subsurface configuration of the batholith in terms of depth and shape in the Archean Metamorphic basement rocks. Figure 18 is the westernmost profile and depicts the

subsurface extent of the batholith SSW to NNE beyond the surface exposure of the contact with the metamorphic basement (Vitaliano and Cordura, 1979). Of the four profiles produced, the westernmost profile has the greatest SSW to NNE lateral extent (16.9 km). This lateral extent and volume suggest that the mass of the batholith extends further to the northwest. The relatively small depth (6.5 km) in Figure 18 compared to the larger depth to the southeast (20 km) in Figure 19 suggests that the subsurface continuation to the northwest is relatively narrow. Figure 19 shows the subsurface extent of the batholith at 15.3 km and a maximum depth of 20 km. The depth of the batholith is greatest in this region of the survey area. The lateral extent of the batholith decreases from Figure 18 (16.9 km) to Figure 19 (15.3 km) suggesting migration from the NW due to a decrease in accommodation space. Figure 20, the eastern central profile, indicates a lateral extent of 9.4 km and maximum depth of 12 km. This is a significant decrease in lateral extent from the 15.3 km (Figure 19) of the batholith to the northwest. It is likely that direction of intrusion of the batholith and separation due to faulting may be the reason for the changes in lateral extent as viewed from NW to SE. The change in depth of 20 km (Figure 19) to 12 km also indicates that as the batholith migrated from the northwest, the amount of accommodation space was decreasing to the southeast. Figure 21, the eastern-most profile, depicts the southeast boundary of the batholith. The subsurface lateral extent for the batholith is at its minimum of 8.6 km. Of the four transects Figure 21 has a minimum depth reaching 3 km. The batholith may extend more towards the southeast, but, if so, the extent is minimal.

To summarize, the simple Bouguer anomaly map, complete Bouguer anomaly map, residual Bouguer anomaly map, and four SW-NE trending transects produce evidence that suggests a rapid decrease in depth and lateral extent from the center

portion of the survey area to the southeast corner and a narrowing of the batholith in the subsurface to the northwest. The narrow subsurface shape on the northwest, parallel to the principal faults, the rapid thickening toward the central region (Figure 19), and the abrupt termination on the southeast (Figure 21) is compatible with magma movement from the northwest, perhaps channeled by major northwest-trending faults and foliation in the metamorphic basement, to a zone of filling restricted to the central part of the batholith. This fits reasonably well the pull-apart model proposed by Schmidt et al. (1990) in which magma was intruded into an expanding zone of diminished pressure in the accommodation space controlled by major northwest-trending faults and influenced by the regional foliation direction in the host metamorphic rocks.

REFERENCES

Bonini, W.E., Smith, R.B., and Hughes, D.W., 1973, Complete Bouguer gravity anomaly map of Montana: Montana Bureau of Mines and Geology, Special Publication 62. Chadwick, R.A., 1972, Volcanism in Montana: Northwest Geology, v. 1, p. 1-20

Burfeind W.J. 1967, A Gravity Investigation of the Tobacco Root Mountains, Jefferson Basin, Boulder batholith, and Adjacent areas of southwestern Montana.

Guineberteau, B., Bouchez, J. L. & Vigneresse, J. L. 1987, The Mortagne granite pluton (France) emplaced by pull-apart along a shear zone: structural and gravimetric arguments and regional implication. Geological Society of America Bulletin, 99, 763-770

Hammer, Sigmund, 1939, Terrain corrections for gravimeter stations: Geophysics, v. 4 no. 3 p. 184-194

Hutton, D. H. W. 1988. Granite emplacement mechanisms and tectonic controls: inferences from deformation studies. Royal Society of Edinburgh, Transactions. 79, 245-255

Klusman, Ronald William. Electron microprobe analysis of feldspars [abs]: Dissert. Abs. Internat., Sec. B., Sci. and Eng., v. 30, no. 11, p. 5102B-5103B, 1970

Pitcher J.L. The Anatomy of a batholith. Geological Society of London Vol. 135. 1978, pp. 157-182

Reynolds, M. W., 1979, Character and extent of basin-range faulting, western Montana and east-central Idaho: RMAG-Utah Geol. Soc. 1979 Basin and Range Symposium, p. 185-193.

Schmidt, C. J., and Garihan, J. M., 1983, Laramide tectonic development of the Rocky Mountain foreland of southwestern Montana: Dnver Colorado, Rocky Mountain Association of Geologists, p. 271-294

Schmidt C.J., Garihan J.M., Role of Recurrent Movement of Northwest-Trending Basement Faults in the Tectonic Evolution of Southwestern Montana. Proceeding of the 6th International Conference on Basement Tectonics, Pages 1-15, 1986

Schmidt, C.J. and Hendrix T. E., Tectonic controls for thrust belt and Rocky Mountain foreland structures in the northern Tobacco Root Mountains-Jefferson Canyon area, southwestern Montana, in Tucker, T. E., ed, Southwest Montana: Montana Geological Society Field Conference and Symposium Guidebook, p. 167-180

Schmidt C.J., O'Neill J.M., Structural Evolution of the Southwest Montana Transverse Zone. Rocky Mountain Association of Geologists, 1982

Schmidt C.J., Smedes H.W., O'Neill J.M., Syncompressional Emplacement of the Boulder and Tobacco Root batholiths (Montana-USA) by pull-apart along Old Fault Zones, 1990

Smith J.L. 1977, Petrology, Mineralogy, and Chemistry of the Tobacco Root batholith, Madison County, Montana. Indiana University Thesis research

Vitaliano, C. J., and Cordua, W. S., 1979, Geologic map of the southern Tobacco Root Mountains, Madison County, Montana: Geological Society of America Map and Chart Series MC-31, scale 1:62,500.

Vitaliano, C. J., Cordua, W. S., Burger, H. R., Hanley, T. B., Hess, D. F., and Root, F. K., 1979, Geology and structure of the southern part of the Tobacco Root Mountains, southwestern Montana: Map summary: Geological Society of America Bulletin, pt. 1, v. 90, no. 8, p. 712-715.

Charles J. Vitaliano, H. Robert Burger III, William S. Cordua, Thomas B. Hanley, David F. Hess and Forrest K. Root, Explanatory text to accompany geologic map of southern Tobacco Root Mountains, Madison County, Montana, Geological Society of America Special Papers 2004;377;247-256 doi: 10.1130/0-8137-2377-9.247

Wooden, J. L., Vitaliano, C. J., Koehler, S. W., and Ragland, P. C., 1978, The late Precambrian mafic dikes of the southern Tobacco Root Mountains, Montana: Geochemistry, Rb-r geochronology, and relationship to Belt Tectonics: Canadian Journal of Earth Sciences. V. 15 p. 467-479

APPENDIX

ALTERNATE GRAVITY MODELS

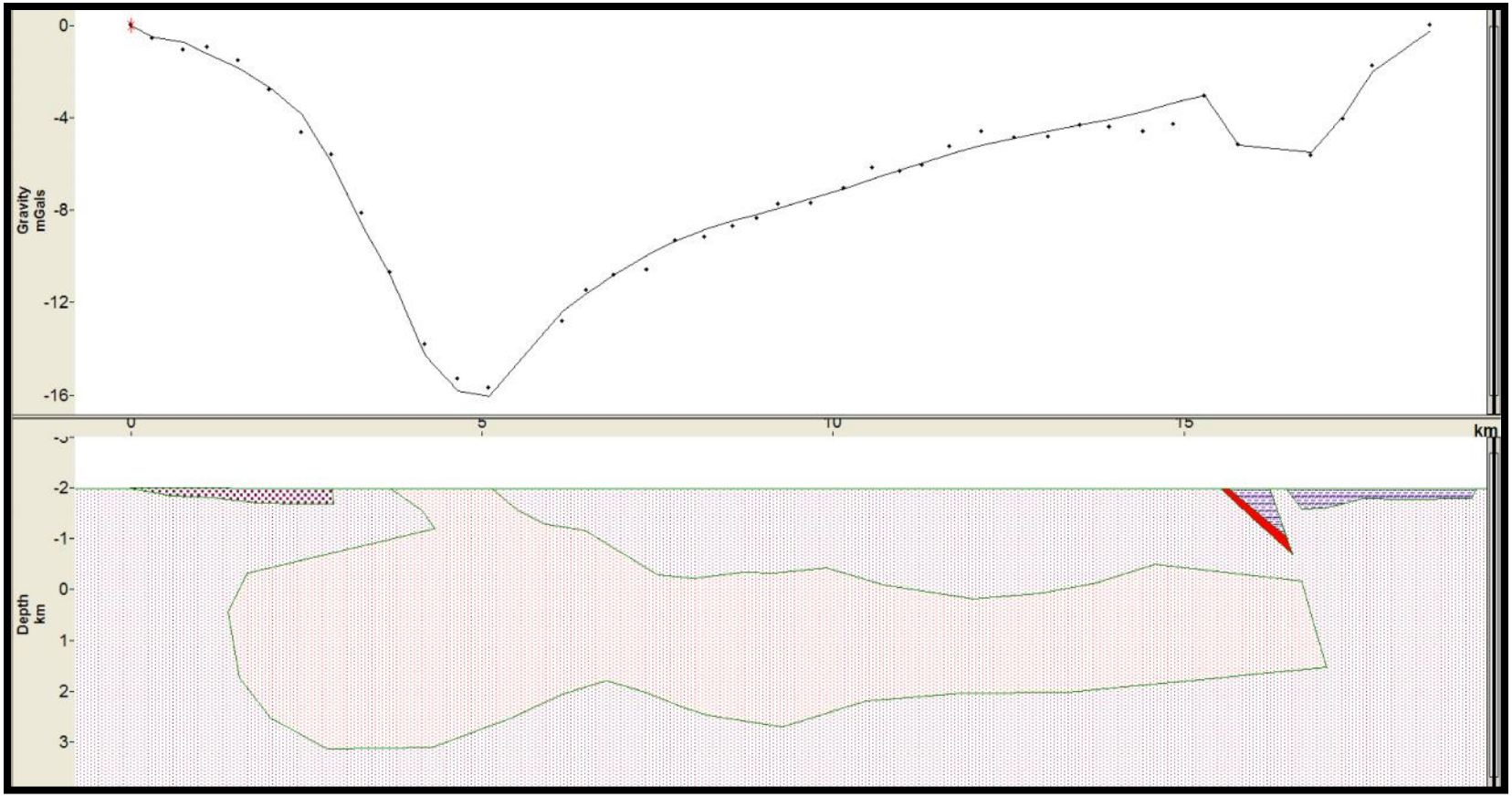

Figure 18a: The west most profile from SW-NE depicts a calculated gravity low of -16 mGal. The homogeneous batholith (red) with an average density of 2.67 g/cm^3 extends 15.75 km in the subsurface reaching 5 km depth from the surface. The surrounding Archean basement rocks (maroon) have an average density of 2.87 g/cm^3 giving a density contrast of 0.20 g/cm^3. The feature located on the SW portion of the profile is hornblende gneiss and granulite mapped by Vitaliano (1979) and was

assigned a density value of 3.1 g/cm^3. The features on the NE portion of the profile are a sill (red) and limestone (purple) and have been assigned density values of 3.0 g/cm^3 and 2.4 g/cm^3, respectively.

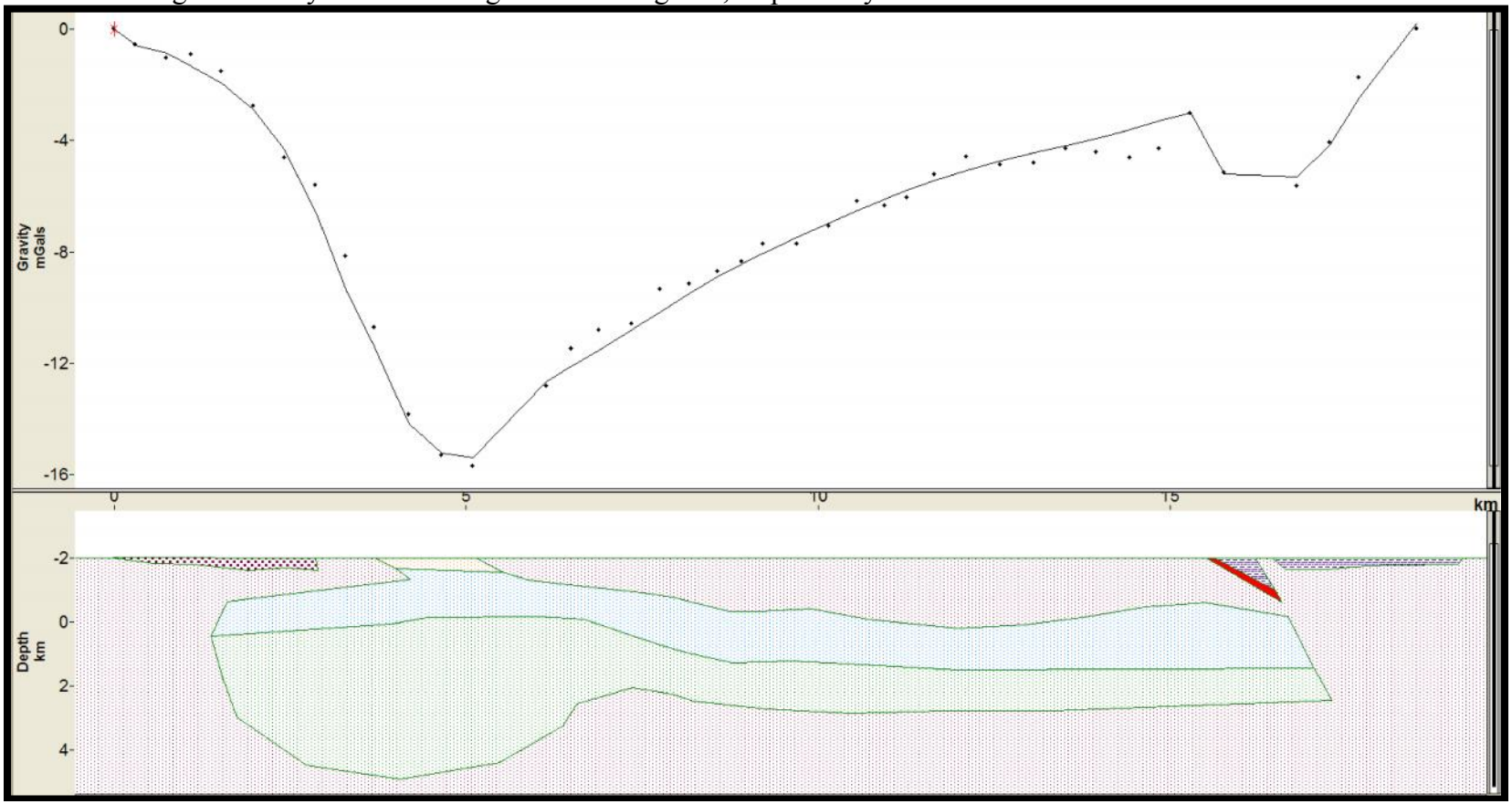

Figure 18b: The west most profile from SW-NE depicts a calculated gravity low of -15 mGal. The zoned batholith consists of hornblende tonalite (orange) with an assigned density of 2.72 g/cm^3, tonalite (blue) with an assigned density of 2.71 g/cm^3, granodiorite (green) with an assigned density of 2.68 g/cm^3, and extends 16.9 km in the subsurface reaching 6.9 km depth from

the surface. The surrounding Archean basement rocks (maroon) have an average density of 2.87 g/cm^3. The feature located on the SW portion of the profile is hornblende gneiss and granulite mapped by Vitaliano (1979) and was assigned a density value of 3.1 g/cm^3. The features on the NE portion of the profile are a sill (red) and limestone (purple) and have been assigned density values of 3.0 g/cm^3 and 2.4 g/cm^3, respectively.

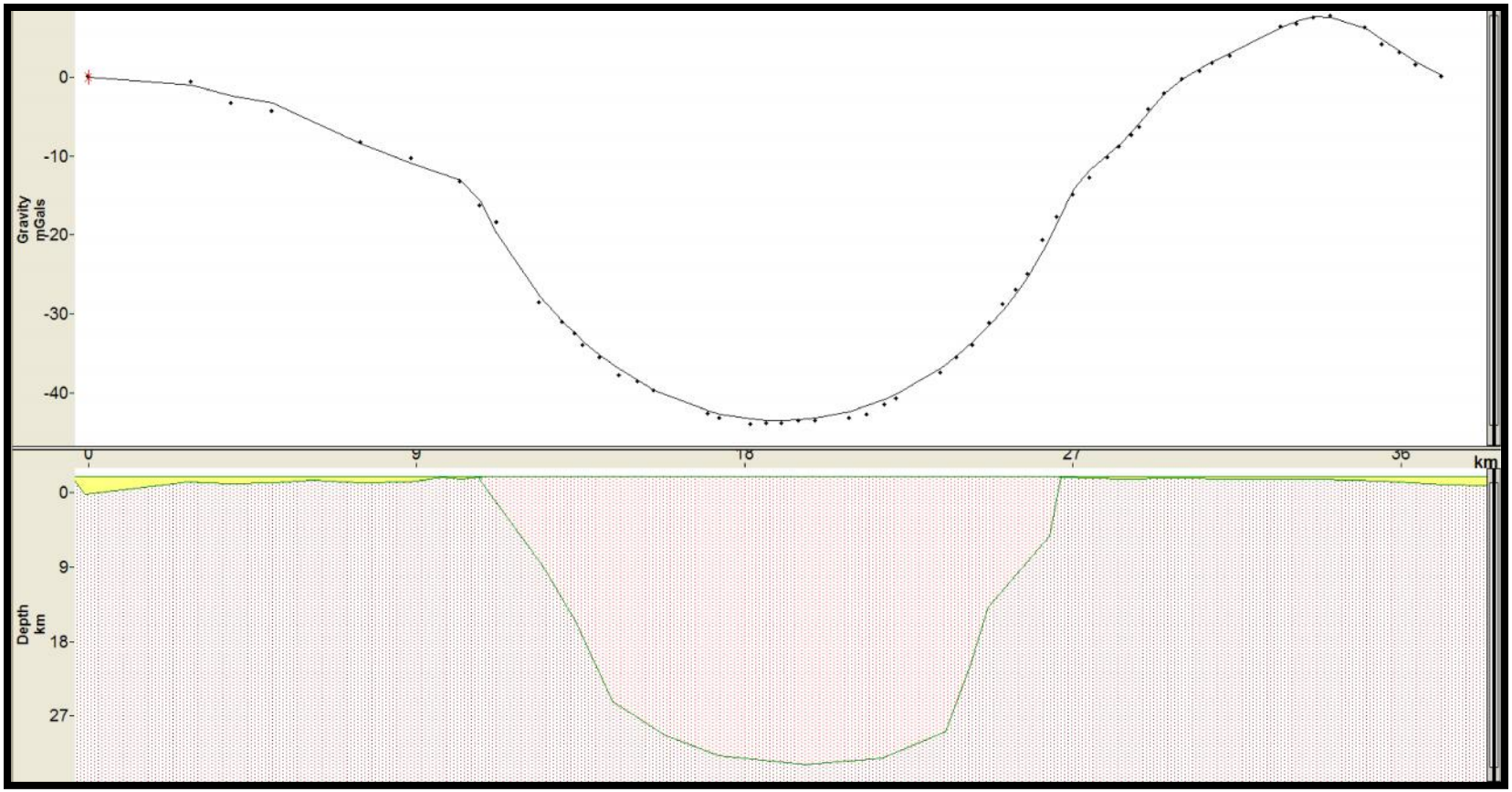

Figure 19a: The west central profile from SW-NE depicts a calculated gravity low of -43 mGal. The homogeneous batholith

(red) with an average density of 2.67 g/cm^3 extends 15 km in the subsurface reaching 35.75 km depth from the surface. The surrounding Archean basement rocks (maroon) have an average density of 2.87 g/cm^3 giving a density contrast of 0.20 g/cm^3. The features located on the SW and NE portion of the profile near the surface are alluvium (yellow) with an assigned density of 2.30 g/cm^3.

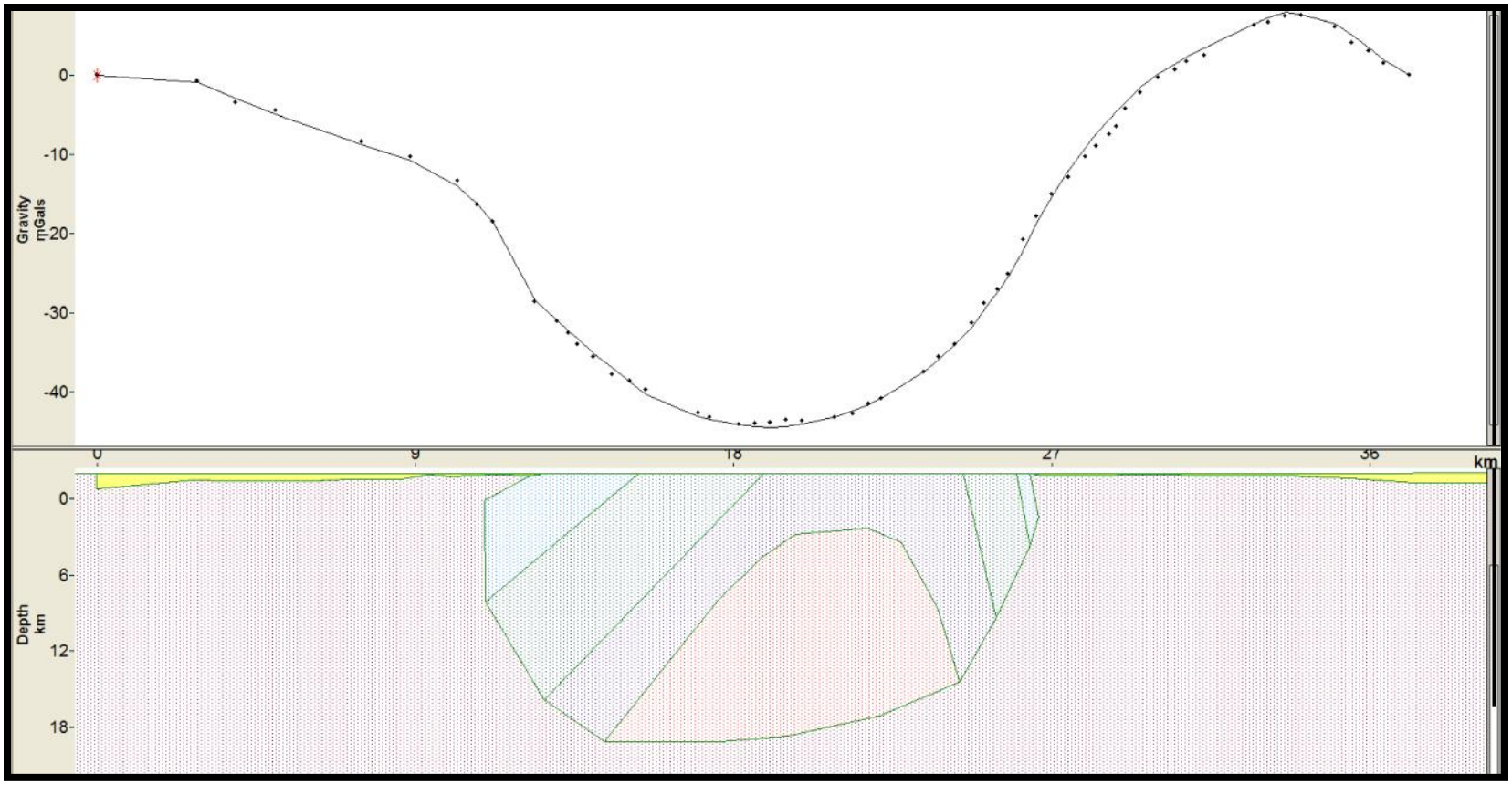

Figure 19b: The west central profile from SW-NE depicts a calculated gravity low of -44 mGal. The zoned batholith consists

of tonalite (blue) with an assigned density of 2.71 g/cm^3, granodiorite (green) with an assigned density of 2.68 g/cm^3, quartzmonzonite with an assigned density of 2.675 g/cm^3, granite with an assigned density of 2.67 g/cm^3, and extends 15.7 km in the subsurface reaching 21 km depth from the surface. The surrounding Archean basement rocks (maroon) have an average density of 2.87 g/cm^3. The features located on the SW and NE portion of the profile near the surface are alluvium (yellow) with an assigned density of 2.30 g/cm^3

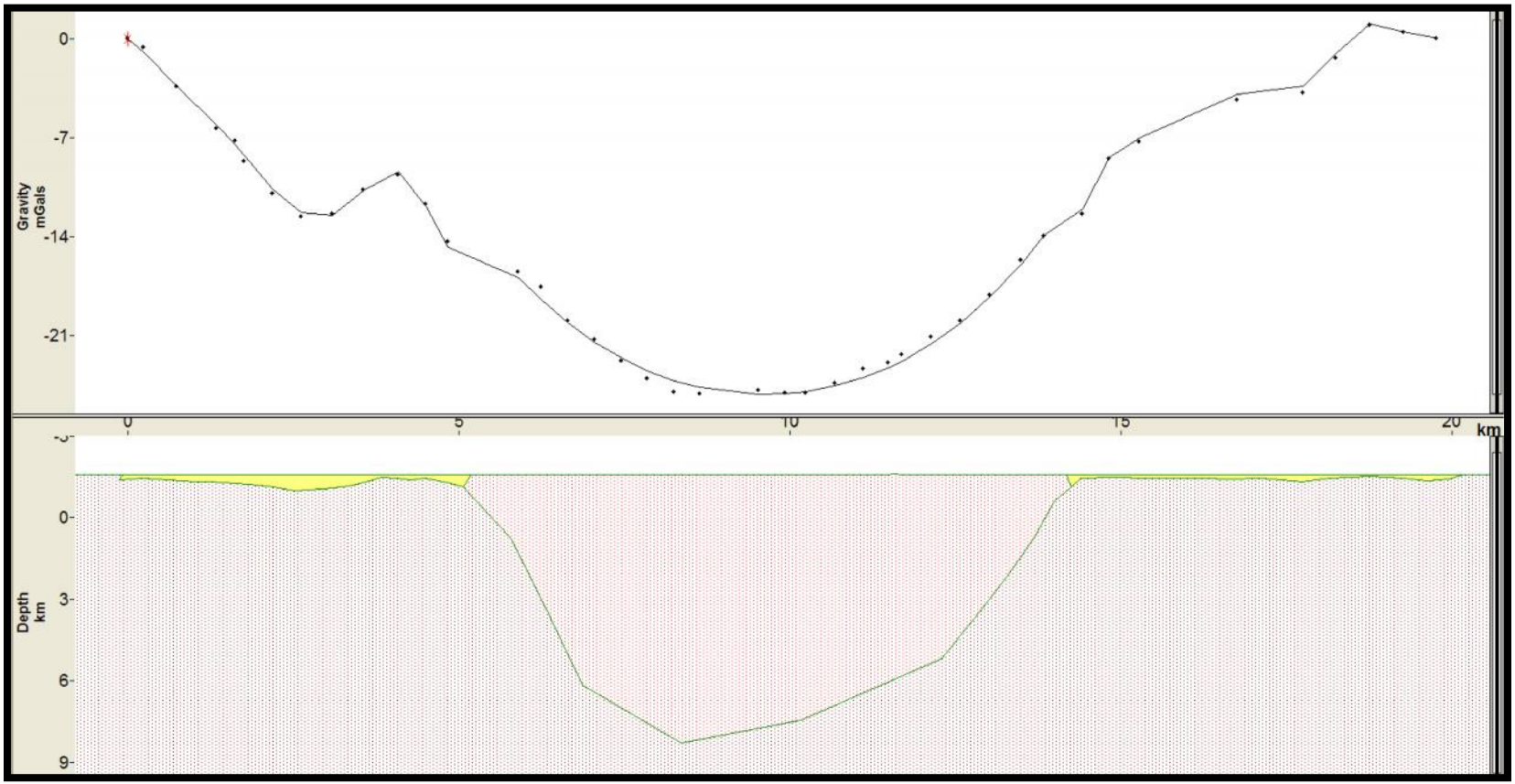

Figure 20a: The east central profile from SW-NE depicts a calculated gravity low of -25 mGal. The homogeneous batholith (red) with an average density of 2.67 g/cm^3 extends 9.2 km in the subsurface reaching 9.85 km depth from the surface. The surrounding Archean basement rocks (maroon) have an average density of 2.87 g/cm^3 giving a density contrast of 0.20 g/cm^3.

The features located on the SW and NE portion of the profile near the surface are alluvium (yellow) with an assigned density of 2.30 g/cm^3.

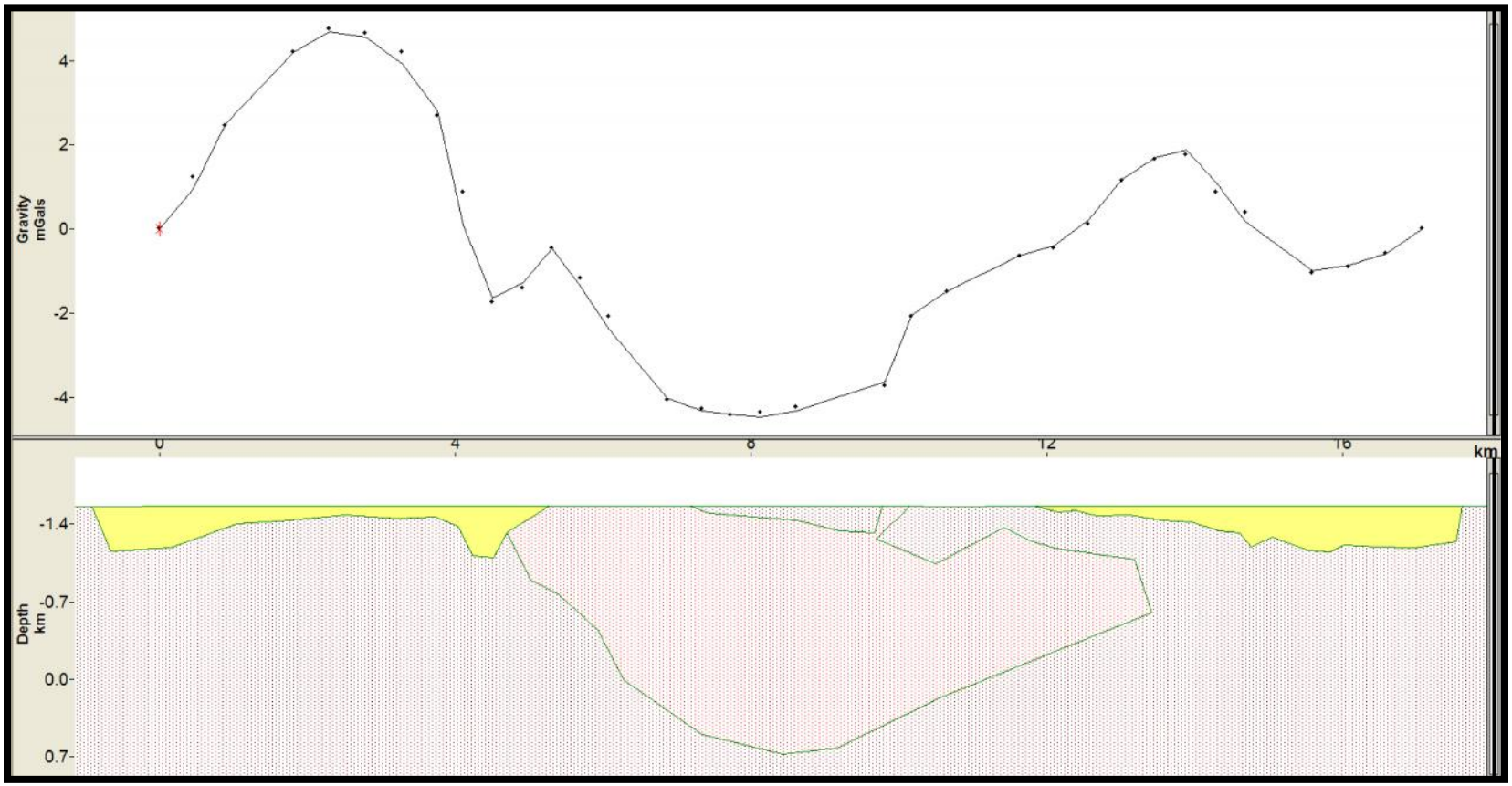

Figure 21a: The east most profile from SW-NE depicts a calculated gravity low of -4 mGal. The homogeneous batholith (red) with an average density of 2.67 g/cm^3 extends 8.8 km in the subsurface reaching 2.2 km depth from the surface. The surrounding Archean basement rocks (maroon) have an average density of 2.87 g/cm^3 giving a density contrast of 0.20 g/cm^3.

The features located on the SW and NE portion of the profile near the surface are alluvium (yellow) with an assigned density of 2.30 g/cm^3.

BIBLIOGRAPHY

Lillie, Robert J. Whole Earth Geophysics: An Introduction Textbook for Geologists & Geophysicists. Pearson-Hall, Inc. 1999

Telford, W. M., Geldart, L. P., Sheriff, R.E. Applied Geophysics Second Edition. Cambridge University Press. 1990